Final Report

ARCTAS-California 2008: An airborne mission to investigate California air quality

CARB Award No. 07-335

Principal Investigator

Donald R. Blake

Professor, Department of Chemistry

University of California, Irvine

Irvine, CA 92697

(949) 824-4195

(949) 824-2905 (FAX)

e-mail: drblake@uci.edu

Report prepared for:

State of California Air Resources Board

Research Division

PO Box 2815

Sacramento, CA 95812

Project Dates: 05/01/2008-05/15/2010

January 2010

Acknowledgements

Samples described in this report were obtained by Julie Lee, Matt Carlson, Marco Orozco, Jim Pederson, Andreas Beyersdorff, and Melissa Yang and were analyzed by Brent Love, Gloria Liu, Simone Meinardi, Barbara Barletta, Paul Nissenson, and Matt Gartner. We are indebted to the pilots and technicians who maintain the NASA DC-8 aircraft.

List of Figures and Tables

List of Tables

Executive Summary

Volatile organic compounds (VOCs) play a primary role in the reaction scheme leading to the formation of tropospheric ozone. During this contract, we were able to measure a wide variety of VOCs over California, focusing on the characterization on the lower troposphere of important source regions such as the San Joaquin Valley (SJV), the Los Angeles (LA) air basin and, in general, the South California air basin (SCAB). The improved knowledge on the speciation of VOCs over California is crucial for the improvement of state emission inventories for greenhouse gases and aerosol, for the characterization of offshore emissions of sulfur and other pollutants from shipping and natural sources, and for the characterization of upwind boundary conditions for modeling local surface ozone and $PM_{2.5}$.

Whole-air samples were collected on board the NASA DC-8 aircraft during several research flights (ARCTAS-CARB study) carried out in June 2008. These samples were analyzed at the University of California, Irvine for more than 75 gases, including nonmethane hydrocarbons, halocarbons, alkyl nitrates, sulfur compounds, and oxygenated compounds.

Among the different halocarbons, we measured several important greenhouse gases such as CFC replacement compounds. We were able to characterize the distribution over California of three HCFCs (HCFC-22, HCFC-142a, HCFC-141a) and two HCFs (HFC-134a and HFC-152a). We focused our attention on the LA basin and on one of the fastest increasing species, namely HFC-152a. Using the data obtained during the flights over the LA air basin we were able to extrapolate the annual emission of HFC-152a and evaluate the role of the United States on the HFC-152a global emissions. We also used an air quality model to validate our results and we found a very good agreement between the emissions predicted by the urban model and the emissions calculated using the observation obtained over the LA basin during the different research flights.

Finally, this contract allowed us to observe the background levels of selected oxygenated compounds over the SJV, and ultimately to evaluate the enhancement of such species through both the east and the west sides of the valley. An assessment of the emissions of the oxygenated compounds in the valley was achieved using data

obtained on board the DC-8 on low altitude flights through the valley. Among these species, we found that ethanol, methanol, and acetaldehyde were produced in major quantities throughout the SJV as by-products of yeast fermentation of silage and photochemical oxidation. These oxygenates play an important role in ozone formation within the valley. Based on our observations, we were able to distinguish between cities versus dairy emission sources.

Disclaimer

The statements and conclusions in this report are those of the authors from the University of California and not necessarily those of the California Air Resources Board. The mention of commercial products, their source, or their use in connection with the material reported herein is not to be construed as actual or implied endorsement of such products.

ABSTRACT

Four research flights on board the NASA DC-8 aircraft were sponsored by the California Air Resources Board (CARB) and carried out over California in June 2008. Among many other measurements, whole air samples were collected by the UC-Irvine (University of California, Irvine) research group in electropolished stainless steel canisters. Once filled, the canisters were shipped and analyzed at the UC-Irvine laboratory for a wide variety of volatile organic compounds (VOCs) including nonmethane hydrocarbons, halogenated species, alkyl nitrates, selected sulphur and oxygenated compounds.

We start with an overview of the VOC levels measured over California, and then focus on two different topics: CFC replacement compounds, and oxigenated species.

HCFCs and HFCs have been introduced as substitute of CFC compounds in response to the regulations imposed by the Montreal Protocol and subsequent amendments. While HCFCs still contribute to the destruction of the stratospheric ozone layer, the chlorine-free compound HFCs do not pose any treat to the ozone layer but are important greenhouse gases enhancing radiative forcing. Using the data collected during the CARB research flights over the Los Angeles area we were able to extrapolate the annual emission of HFC-152a, one of the fastest increasing CFC replacement compounds measured.

Finally, we were able to determine the background and enhanced levels of selected oxygenated compound in the San Joaquin Valley.

1. INTRODUCTION

The NASA Arctic Research of the Composition of the Troposphere from Aircraft and Satellites (ARCTAS) study was conducted in two different deployments (April 2008 – ARCTAS-A; and June-July 2008 – ARCTAS-B) involving the DC-8, P-3 and B-200 aircrafts characterized by different payloads. Before the second deployment, four research flights on board the DC-8 aircraft were sponsored by CARB and carried out over California in June 2008. The objectives of the California deployment (ARCTAS-CARB) were to: (1) improve state emission inventories for greenhouse gases and aerosols; (2) characterize offshore emissions of sulfur and other pollutants from shipping and natural sources; and (3) characterize upwind boundary conditions for modeling local surface ozone and $PM_{2.5}$.

Among the different measurements, whole air samples were collected on board the DC-8 and analyzed for selected volatile organic compounds (VOCs). The importance and role of VOCs on the formation of tropospheric ozone is well known as ozone is produced in the troposphere by the oxidation of VOCs in the presence of sunlight and nitrogen oxides (NO_x=NO+NO_2). Many of the measured halogenated compounds presented here are also regulated under the Montreal Protocol and its subsequent amendments because of their potential to deplete stratospheric ozone (WMO, 2002; UNEP, 2003). HCFCs and HFCs have been introduced as substitute of CFC compounds in response to the regulations imposed by the Montreal Protocol and subsequent amendments. While HCFCs still contribute to the destruction of the stratospheric ozone layer, the chlorine-free compound HFCs do no pose any treat to the ozone layer. However, because of their ability to absorb infrared radiation, HFCs are important greenhouse gases enhancing radiative forcing.

Through the analysis of the data set obtained during the ARCTAS-CARB deployment we characterized the VOC composition in different source regions within the South Coast Air Basin (SCAB) and in the San Joaquin Valley (SJV). In particular, we present the distribution of the halocarbon fraction measured over California (focusing on the LA Basin in particular) in response to one of the main objective of the ARCTAS-CARB mission (i.e. provide observations to improve emission inventories for greenhouse gases).

We also gained a better overall understanding of the impact of dairy emissions on the air quality in the SJV through the study of four oxygenated compounds measured during our sampling.

We expect that the ARCTAS-CARB data will provide an important foundation for improving models of air quality and greenhouse gas emissions in California.

2 BACKGROUND

2.1 Air pollution and tropospheric ozone production

Air pollution is a major problem in many urban areas around the world. Long-range transport of pollutants can affect areas far away from their source, making urban air pollution a regional and global issue. The main effects of air pollution include damage of materials and vegetation, visibility degradation, and most importantly, adverse affects on human health.

Among the different chemical compounds emitted into the troposphere as a result of human activities, NO_x and VOCs are particularly important because the chemical reactions involving these species and hydroxyl radicals (OH) in the presence of sunlight and sufficiently warm temperatures (>18°C), lead to the formation of tropospheric ozone.

Ozone is a well-recognized greenhouse gas (Berntsen *et al*., 1997; IPCC, 2001; Shine, 2001), a toxic compound, and one of the six criteria pollutants. Ozone is also one of the key components of the "greenhouse effect", because is a direct greenhouse gas (GHG) and because it indirectly modifies the lifetime of other GHGs, methane (CH_4) being the most important. Ozone levels in the troposphere can range between about 20-40 part per billion by volume (ppbv) in remote areas not affected by direct anthropogenic activities (Vingarzan, 2004), while in polluted urban areas O_3 levels can exceed 100 ppbv (Daum *et al*., 2004; Kleinman *et al*., 2002).

The only known reaction leading to the formation of tropospheric ozone involves the photolysis of nitrogen dioxide (reactions 1-3). Ozone is then rapidly consumed in the subsequent reaction of NO, which regenerates NO_2 (reaction 3):

$$NO_2 + h\nu \rightarrow NO + O(^3P) \qquad (280 < \lambda < 430\ nm) \qquad (1)$$

$$O(^3P) + O_2 + M \rightarrow O_3 + M \qquad (2)$$

$$NO + O_3 \rightarrow NO_2 + O_2 \qquad (3)$$

The third body molecule M in reaction (2) is needed to remove the excess energy of the reaction and stabilize ozone. This cycle establishes a steady-state ozone concentration leading to no net formation or loss of ozone. Net ozone formation occurs when VOCs are considered. The most important physical processes involving VOCs are wet and dry deposition, while photolysis and reaction with OH, O_3, and NO_3 are the main chemical transformations. Nitrate radicals have a strong absorption in the visible region of the spectrum, and therefore can only play a role in nighttime chemistry. Chlorine and bromine atoms (Cl, Br) are also involved in VOC degradation. However, because of their generally low concentration in the global troposphere, chlorine and bromine chemistry is believed to be minor and limited to isolated situations. Hydroxyl radicals are the most important oxidizing radicals involved in tropospheric VOC degradation. The reactions considered the major pathways in a generic VOC oxidation are here summarized:

$$RH + OH \rightarrow R\cdot + H_2O \quad (4)$$

$$R\cdot + O_2 + M \rightarrow ROO\cdot + M \quad (5)$$

$$ROO\cdot + NO \rightarrow RO\cdot + NO_2 \quad (6)$$

$$RCH_2O\cdot + O_2 \rightarrow RCHO + HO_2\cdot \quad (7)$$

$$HO_2\cdot + NO \rightarrow OH + NO_2 \quad (8)$$

Because of the presence of VOCs (emitted either by a natural or anthropogenic source), NO molecules are oxidized to NO_2 via $ROO\cdot$ or $HO_2\cdot$ reactions rather than via consumption of O_3 (see reaction 3 in the NO/O_3 cycle represented by reactions 1-3).

2.2 VOC Sources

Volatile organic compounds are emitted from both anthropogenic and biogenic sources. The most important anthropogenic sources are stationary fuel-related (combustion from power plants, extraction and handling of fossil fuels, service stations, emissions from fuel storage), transport-related (vehicular and evaporative emissions) and industrial (mainly solvent use, solvent storage, and transport). Anthropogenic emissions of oxygenated VOCs are trivial compared to biogenic sources (Singh *et al*., 2004). Methyl iodide, methyl chloride, methyl bromide, bromoform, dimethyl sulfide, and C_1-C_2 alkyl nitrates have significant oceanic emissions (Atlas *et al*., 1993; Quack and Wallace, 2003: Swanson *et al*., 2004).

Mobile sources

Among the different anthropogenic sources, energy-related emissions of nonmethane hydrocarbons (NMHCs), a major VOC sub-class, dominate, with vehicular emissions being by far the most dominant combustion sources. The majority of NMHCs released in urban areas are the result of incomplete combustion of fuel, direct formation during combustion, or release of unburned gasoline. Gasoline is the dominant fuel for light and medium-duty road vehicles, which represent the majority of the motor vehicle fleet. The major VOCs emitted by mobile sources are listed here:

- CO, ethyne, short chain alkenes (i.e. ethene, *iso*-butene, 1,3-butadiene), and aromatic compounds are the main gases emitted by motor vehicles as result of incomplete combustion of fuels or the combustion process itself.
- Relatively short chain alkanes are most abundant in gasoline exhaust (as an unburned component) while longer chain alkanes are the most abundant unburned gases in diesel exhaust (Watson *et al*., 2001).
- Long chain alkane emissions (C_4 and higher) are associated with gasoline evaporation (evaporation of liquid fuel from vehicles) and unburned fuel. *n*-Butane, *i*-butane, and *i*-pentane are the major components of the evaporated gasoline due to their low volatility. *i*-Pentane is also commonly found in the exhaust emissions, mainly as an unburned component.

Stationary-fuel-related sources

A significant portion of VOCs is emitted by stationary fuel-related sources such as power plants and petroleum refineries (Placet *et al*., 2000). Refueling emissions at filling stations, emissions from underground storage of gasoline at filling stations, and leakage from LPG and natural gas used for cooking and heating also contribute to the total VOC emissions from stationary sources.

Alkanes (mainly C_2-C_8 linear alkanes), aromatics (benzene, toluene, *m*- and *p*-xylene, and ethylbenzene), and short chain alkenes (ethene and propene) are often the most abundant species measured around petroleum refineries (Lin *et al*., 2004). These gases overlap with most of the NMHCs emitted by mobile sources.

Light alkanes (C_1-C_4) are mostly emitted by LPG or natural gas leakage.

Most of the compounds emitted by mobile sources (i.e. CO, alkenes, aromatics) are also emitted by biomass/fuel burning. However, some gases are considered specific trace gases for biomass burning. For example, methyl chloride (CH_3Cl) has strong

natural sources, but biomass and biofuel burning, including coal burning, are major anthropogenic sources (Blake *et al*., 1996; McCulloch *et al*., 1999).

Industrial sources

Nonmethane hydrocarbons and halogenated compounds, representing a major fraction of VOCs, both have strong industrial sources.

- Chlorofluorocarbons (CFCs) were first introduced as nontoxic and nonflammable refrigerants in cooling appliances in the 1930s, but they also found application as foam blowing agents, in air conditioning, and as aerosol propellants (McCulloch *et al*., 2001; Sturrock *et al*., 2002). CFC-11 together with CFC-113 was also used as degreasing agents. Because of the implementation of the Montreal Protocol (1987) and subsequent amendments, CFCs have been replaced by hydrochlorofluorocarbons (HCFCs) such as HCFC-22, HCFC-141b, and HCFC-142b and more recently by the hydrofluorocarbon (HFC). HCFCs and HFCs are mainly emitted from refrigeration units, air conditioning units or foam plastic applications (McCulloch *et al*., 2003).
- Several other halogenated compounds have (or had) applications in the industrial sector, mainly as solvents and degreasers, i.e. tetrachloroethene (C_2Cl_4), trichloroethene (C_2HCl_3), 1,1,1-trichloroethane (CH_3CCl_3, methyl chloroform), and dichloromethane (CH_2Cl_2, methylene chloride).
- While benzene is a general combustion tracer (Hellen *et al.*, 2005), toluene, ethylbenzene and the xylenes are used extensively as industrial solvents and for painting.

2.3 Air Quality in California – San Joaquin Valley

Despite extensive abatement efforts, air quality standards are widely exceeded in southern California and the Central Valley.

The federal eight-hour ozone standard is currently set at 0.080 ppm while California's 2005 eight-hour ozone standard is set at 0.070 ppm (Lindberg, 2007). On March 12th, 2008, the EPA strengthened its NAAQS for ground-level ozone to an attainment of 0.075 ppm (USEPA, May 2009). California has its own eight-hour ozone standard as California law authorizes the California Air Resources Board to set its own ambient air pollution standards unique to California, in consideration of public health, safety and welfare (Smith, 2008).

In the SJV, the average number of days exceeding the federal 8-hour ozone standard has declined nearly 20 percent between 1996 and 2006, but maximum levels

have been fairly consistent over the last 10 years, with the average 8-hour value declining by only three percent (CPSJV, 2007). The current deadline to attain the federal 8-hour ozone standard is 2013, with a possibility of extending it to a later attainment year (CPSJV, 2007). To better grasp the problem of pollution in the valley, it is important to realize that the problem is confounded by several other factors besides just emissions alone. These include topography, climate conditions and geography. Figure 1 is an image of the Central valley, highlighting important topographic and geographic features.

Figure 1. Topographical features of the San Joaquin Valley, CA (© 2004 Matthew Trump).

The San Joaquin Valley air basin is approximately 240 miles long, extending parallel to the Pacific Ocean coastline. The central valley has no surface drainage basin to the ocean and endures climatological extremes.

Another factor contributing to the pronounced climatic conditions in the valley is the continuous mixing between maritime and continental air masses as the valley sits in an area of transition, where the conditions are affected by both oceanic and continental influences. The topography of the valley also greatly affects wind movement in and out of the valley basin. California sits in an area of prevailing westerlies and is on the east

side of the semi-permanent high pressure area of the northeast Pacific Ocean. The general flow of air throughout the state is from northwest throughout the year. However, due to the topography of the state, a lot of the air is deflected resulting in wind direction driven by local terrain instead of prevailing circulation. This phenomenon is very pronounced within the San Joaquin valley. The valley experiences low, regional air evacuation and dispersion rates that are accompanied by frequent inversions, abundant sunlight and extreme temperatures.

Until recently, most of the ozone problem in the central valley was attributed to diesel exhaust emissions associated with the agricultural industry (McDaniel, 2005). In 2006, heavy-duty diesel trucks were identified as the number one source of NO_x emissions, while livestock waste was identified as the second greatest source of VOCs in the valley (Hafer, 2006). The San Joaquin valley is not only the most productive agricultural region in US but in the world (Stoddard, 2009).The valley produces grapes, cotton, nuts, citrus and all types of vegetables. Cattle and sheep are also of importance in the valley with the valley hosting the largest meat lot west of the Mississippi River and with 7 out of 8 counties in the valley being the top milk producing counties in the Country.

The San Joaquin valley is currently home to about 2.5 million cattle (Crow *et* al., 2005). The cow population is expected to increase by another 0.4 million in the next 7 years due to new dairy operations (Owen, 2005). For the past twenty years, manure and the storage lagoons have been cited as the most important air pollution sources found on a dairy farm. One of the goals of our study was to determine if this was in fact true for trace gases.

3. ANLYSIS OF VOLATILE ORGANIC COMPUNDS

3.1 VOC analysis

During the sampling campaign evacuated 2 L electropolished stainless steel canisters were used to collect air samples.Once filled, the canisters were shipped to our laboratory at the University of California, Irvine where—within 7 days of sample collection—they were analyzed for more than 75 gases, including nonmethane hydrocarbons, halocarbons, alkyl nitrates and sulfur compounds.

A detailed description of the analytical system is described in Colman *et* al. (2001). Briefly, a sample amount of 2440 $\pm$ 3 cm^3 (STP) of the air was preconcentrated in a stainless steel loop filled with glass beads and submerged in liquid nitrogen. The sample was then heated to about 80°C, injected, and split into five different column/detector

combinations using UHP helium as the carrier gas. Figure 2 illustrates the schematic of the manifold of the analytical system used to analyze halocarbons and NMHCs.

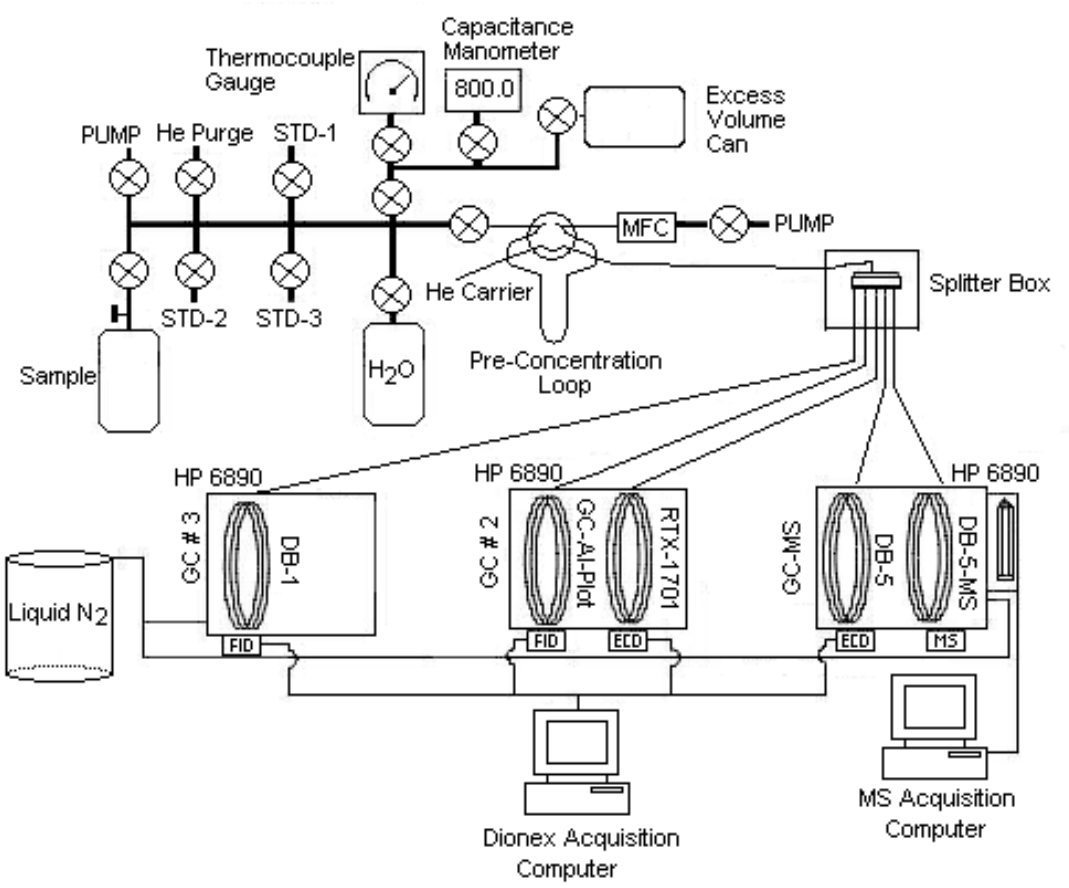

Figure 2. Manifold of the VOC analytical system.

3.2 Columns / Detectors descriptions

The first column detector combination is a DB-1 column (J&W; 60 m, 0.32 mm I.D., 1 µm film thickness) output to a flame ionization detector (FID). The DB-1 column is composed of 100% dimethyl polysiloxane. This column, defined as non polar, when coupled with an FID allows for the identification and quantification (in our experimental conditions) of hydrocarbons with a number of carbon atoms ranging from C_3 to C_{10}. Other compounds of interest quantified with this specific set up are oxygenated molecules and methyl chloride.

The second is a DB-5 column (J&W; 30 m, 0.25 mm I.D., 1 μm film thickness) column connected in series to a RESTEK 1701 column (5 m, 0.25 mm I.D., 0.5 μm film thickness) and output to an electron capture detector (ECD). The DB-5 column is composed of 95% dimethylpolysiloxane and 5% of Phenyl-methylpolysiloxane. This column is non polar and when coupled with an ECD allows the identification and quantification (in our experimental conditions) of halocarbons and alkyl nitrates, and in particular a complete resolution of the methylchloroform and carbon tetrachloride peaks is achieved. Five meters of RESTEK 1701 column are added through a stainless steel internal union (Valco; 1/32", Model ZU.5) in order to obtain a better resolution of some of the alkyl nitrates peaks.

The third is a RESTEK 1701 column (60 m, 0.25 mm I.D., 0.50 μm film thickness) output to an ECD. This column is composed of 14% cyanophenylpropyl / 86% dimethyl polysiloxane and, defined as intermediate polar, when coupled with an ECD allows for the identification and quantification (in our experimental conditions) of halocarbons and alkyl nitrates. In particular C_2 to C_5 alkyl nitrates are better resolved and quantified by this column.

The fourth combination is a PLOT column (J&W GS-Alumina; 30 m, 0.53 mm I.D.) connected in series to a DB-1 column (J&W; 5 m, 0.53 mm I.D., 1.5 μm film thickness) and output to an FID. The Alumina Plot column is composed of Al_2O_3 particles of different deactivation and is used for the resolution of hydrocarbons isomers (in our experimental setup a very good resolution and selectivity for C_2-C_5 hydrocarbons is achieved). This column is highly affected by the amount of CO_2 present in the sample that tends to elute between propane and propene. In order to "move" the CO_2 peak between the two C_3 hydrocarbons mentioned above, 5 m of a DB-1 column are added through a stainless steel internal union (Valco; 1/32", Model ZU.5) at the end of the PLOT column. The DB-1 column also reduces the amount of alumina particles from reaching the FID detector that would result in an increased noise of the baseline.

The final combination is a DB-5ms column (J&W; 60 m, 0.25 mm I.D., 0.5 μm film thickness) output to a quadrupole mass spectrometer detector (MSD, HP 5973). The DB-5ms column is composed of 95% dimethylpolysiloxane and 5% (Phenyl arylene) equivalent to 5% of Phenyl-methylpolysiloxane. This column, defined as a non polar, when coupled with a quadrupole MSD allows for the identification and quantification (in our experimental conditions) of selected hydrocarbons, halocarbons, alkyl nitrates, and

sulfur compounds. The column stationary phase is designed to operate with reduced bleed compared to the DB-5 column.

The MSD was set to operate in selected ion monitoring (SIM) mode with one ion chosen to quantify each compound in order to achieve the maximum sensitivity and to avoid potential interferences. All of the gas chromatographs and detectors used for this project were manufactured by Hewlett Packard.

Table 1 summarized the species that were detected and quantified during the ARCTAS-CARB study.

Table 1. Gases measured and quantified during the ARCTAS-CARB campaign.

Sulphur compounds	**Alkyl nitrates**	**alkynes**
OCS	MeONO2	Ethyne
DMS	EtONO2	Propyne
Halogenated compounds	i-PrONO2	**aromatics**
CFC-12	n-PrONO2	Benzene
CFC-11	2-BuONO2	Toluene
CFC-113	3-PeONO2	Ethylbenzene
CFC-114	2-PeONO2	m+p-Xylene
H-1211	3-Me-2-BuONO2	o-Xylene
H-2402	**Alkanes**	n-Propylbenzene
H-1301	Ethane	3-Ethyltoluene
HCFC-22	Propane	4-Ethyltoluene
HCFC-142b	i-Butane	2-Ethyltoluene
HCFC-141b	n-Butane	1,3,5-Trimethylbenzene
HFC-134a	i-Pentane	1,2,4-Trimethylbenzene
HFC-152a	n-Pentane	1,2,3-Trimethylbenzene
CHCl3	n-Hexane	**Terpene**
CH3CCl3	n-Heptane	alpha Pinene
CCl4	2+3-Methylpentane	beta Pinene
CH2Cl2	2,3-Dimethylbutane	**heterocyclic compound**
C2HCl3	**Alkenes**	Furan
C2Cl4	Ethene	**Oxygentated compounds**
CH3Cl	Propene	Methanol
CH3Br	1-Butene	Ethanol
CH3I	i-Butene	Acetone
CH2Br2	trans-2-Butene	Methyl Ethyl Ketone -MEK

CHBrCl2	cis-2-Butene	Methacrolein -MAC
CHBr2Cl	1,3-Butadiene	Methyl Vinyl Ketone -MVK
CHBr3	Isoprene	Methyl Tert-Butyl Ether -MTBE
Ethyl Chloride		
1,2-Dichloroethane		

3.3 Accuracy, precision, limit of detection.

The analytical accuracy ranges from 2 to 20%, and the precision of the measurements vary by compound and by mixing ratio. For instance, the measurement precision is 1% or 1.5 pptv (whichever is larger) for the alkanes and alkynes, and 3% or 3 pptv (whichever is larger) for the alkenes. The precision of the halocarbon measurements also varies by compound and is 1% for the CFCs and CCl_4; 2-4% for the HCFCs; 5% for HFC-134a and CH_2Cl_2; and 2% for Halon-1211, methyl halides, CH_3CCl_3, C_2Cl_4, and $CHBr_3$. The measurement accuracy also varies by compound and is 2% for CFCs (except 5% for CFC-114); 10% for the HCFCs, C_2Cl_4, CH_2Cl_2, CH_3I and $CHBr_3$; and 5% for Halons, HFC-134a, CH_3CCl_3, CCl_4, CH_3Cl, CH_3Br, and hydrocarbons.

The original standard for the calibration of the NMHCs was gravimetrically prepared from National Bureau of Standards and Scott Specialty Gases standards (accuracy $\pm$ 5%). These standards were used for the calibration of highly pressurized whole air standards (2000 psi) contained within aluminum cylinders. The air was then transferred from the cylinder to an electropolished stainless steel pontoon (34 L) equipped with a Swagelok metal bellows valve, after the initial addition of 15 Torr of degassed ultrapure MilliQ water. A higher degree of stability inside the pontoon has been determined for higher molecular weight hydrocarbons, alkyl nitrate, sulfur species and some of the halocarbons. During the analysis a working standard was analyzed every eight samples, and once a day a series of different standards, including primary standards, were analyzed.

4. FIELD MEASUREMENTS

4.1 Collection of air samples

Samples were collected in 2-L electropolished stainless steel canisters equipped with a Swagelok metal bellows valve. Prior to shipping to the field the canisters were flushed with ultra-high purity (UHP) helium and subsequently evacuated to 10^{-2} Torr in the

laboratory at the University of California, Irvine (UC-Irvine). Seventeen Torr of degassed ultrapure MilliQ water were added to the canisters in order to passivate the surface of the internal walls, so that the absorbance of selected compounds inside the canisters would be minimized. During the sampling the canisters were pressurized to 40 psi using a metal double bellows pump. The filling time was approximately one minute. Canisters were filled at 1-3 minute intervals during ascents and descents, and every 2-8 minutes during horizontal flight legs. A maximum of 168 canisters were filled for each flight on the DC-8.

4.2 Geographical distributions of air samples

During the ARCTAS-CARB deployment a total of 617 whole air samples were collected on board the DC-8 during the 4 science flights (flights # 12-15). In our data analysis, we also make use of 306 samples collected during the transit flight to Cold Lake for the second ARCTAS deployment (flight # 16 on June 26, 2008 – 142 samples) and the final transit from Cold Lake to California on July 13, 2008 (flight # 24 – 164 samples). During the transit flights low altitude passes over the San Joaquin Valley were carried out by the DC-8.

Figure 3 illustrates the geographical location of all the samples; while Figures 4-9 illustrate the position of the samples collected during the individual research flights.

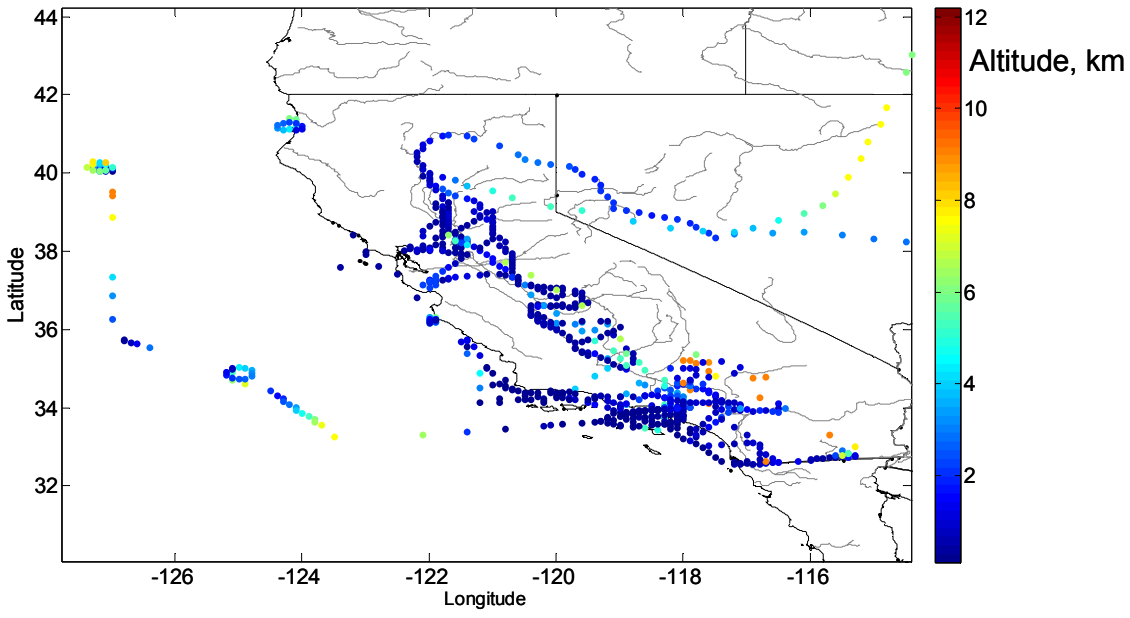

Figure 3. Geographical location of the samples collected during the four ARCTA-CARB flights and the two transit flights to and from Cold Lake (Canada). The samples are color-coded by altitude.

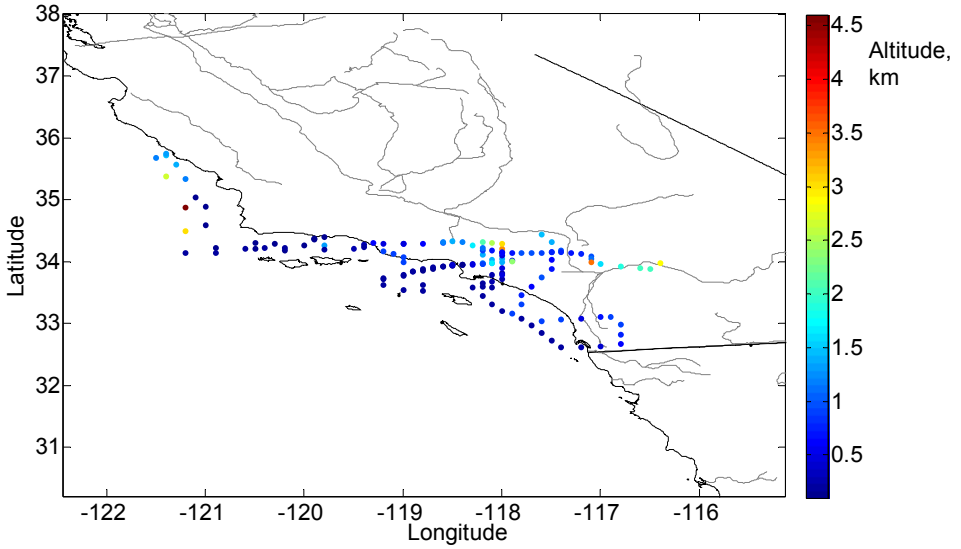

Figure 4. Samples collected on June 18, 2008 during the first CARB flight (flight #12). The samples are color-coded by altitude.

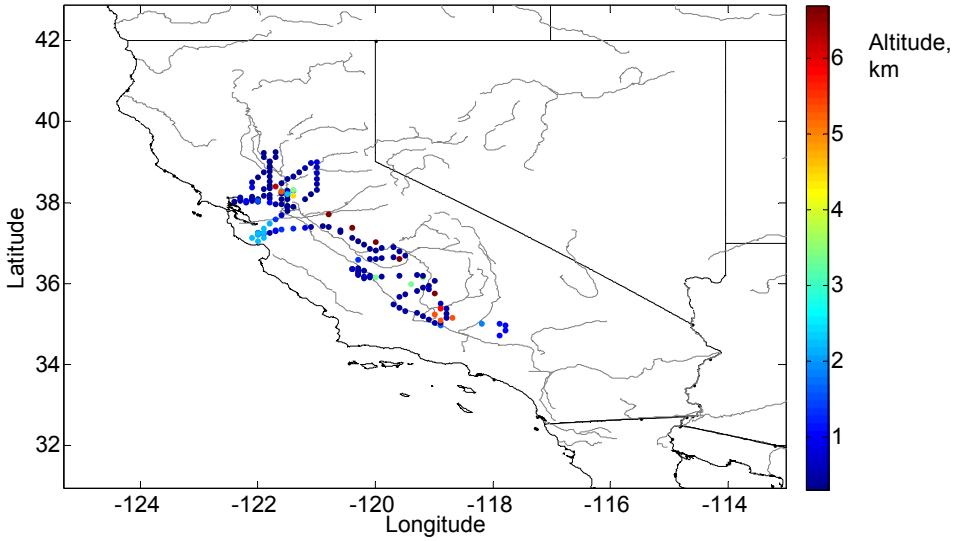

Figure 5. Samples collected on June 20, 2008 during the first CARB flight (flight #13). The samples are color-coded by altitude.

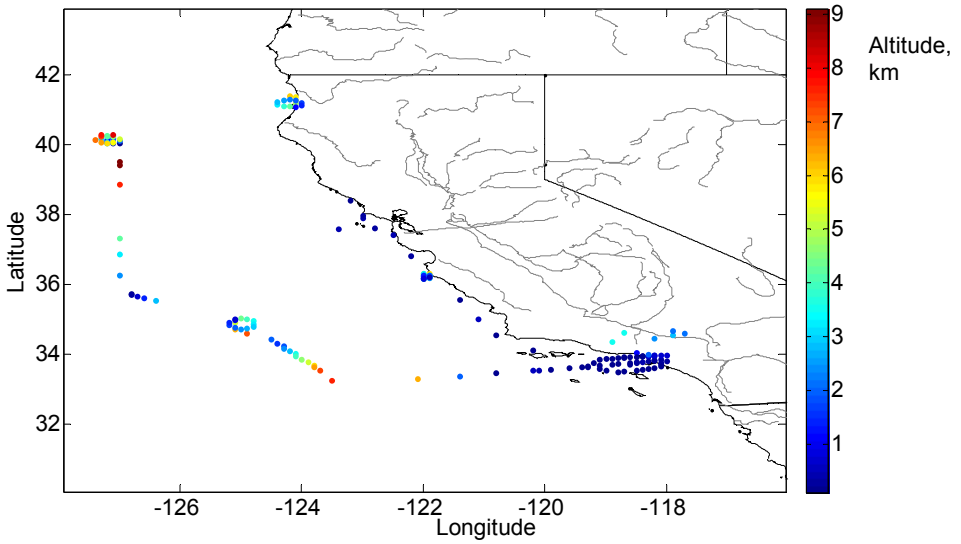

Figure 6. Samples collected on June 22, 2008 during the first CARB flight (flight #14). The samples are color-coded by altitude.

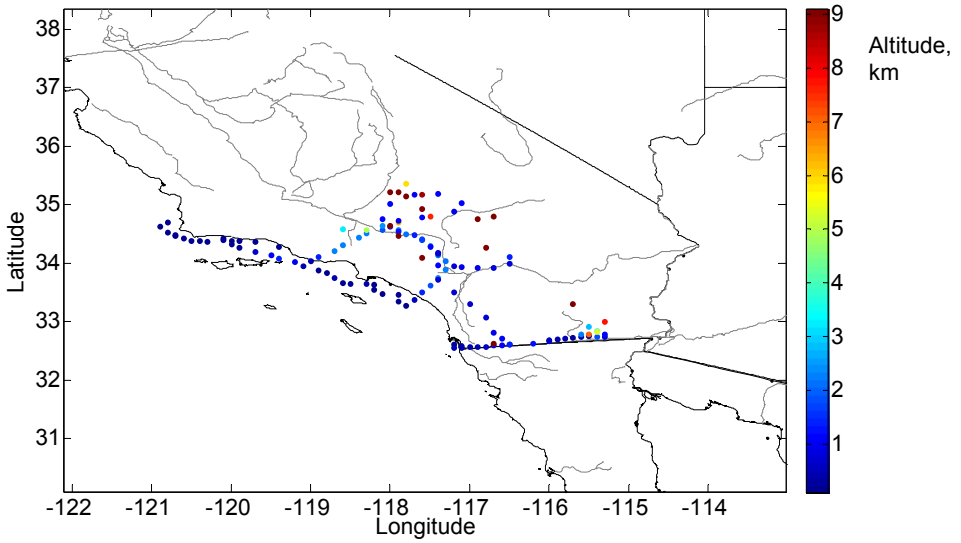

Figure 7. Samples collected on June 24, 2008 during the first CARB flight (flight #15). The samples are color-coded by altitude.

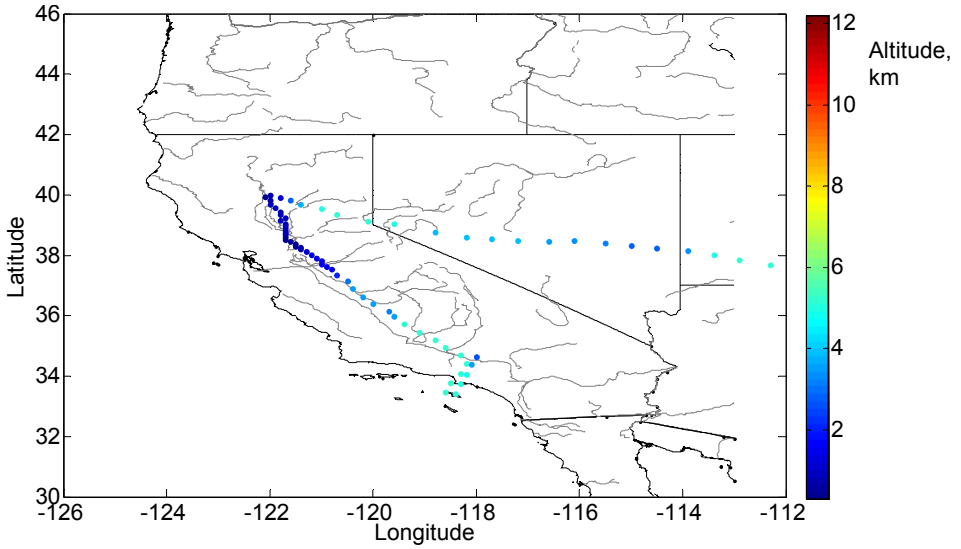

Figure 8. Samples collected on June 26, 2008 during the first flight of the second ARCTAS deployment (flight #16 – transit to Cold Lake, Canada). The samples are color-coded by altitude.

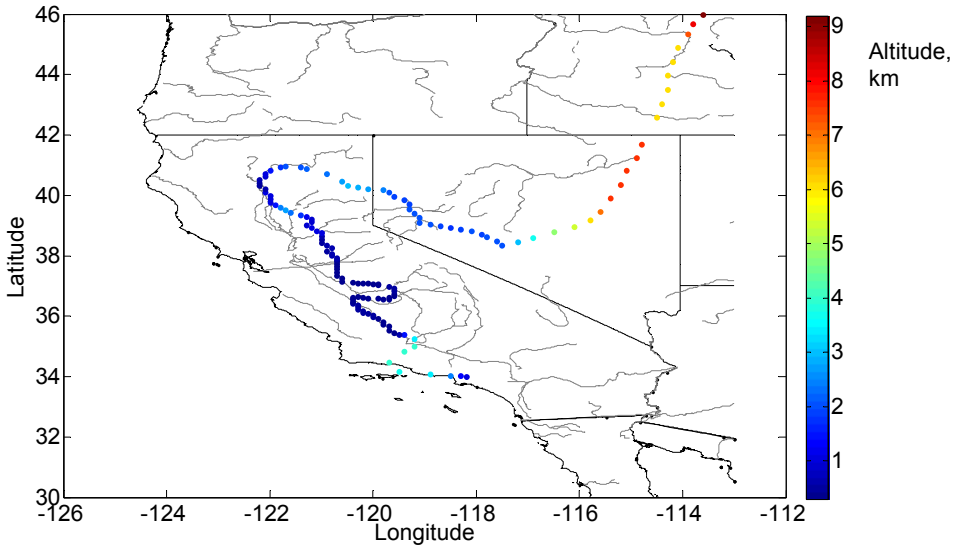

Figure 9. Samples collected on July 13, 2008 during the last flight of the second ARCTAS deployment (flight #24 – transit back to California). The samples are color-coded by altitude.

5. RESULTS

5.1 General features

To show the general trends of the VOCs measured during the ARCTAS-CARB mission (research flights 12-15), the vertical profiles of ethyne (C_2H_2), benzene, tetrachloroethene (C_2Cl_4), and HFC-134a measured on board of the DC-8 aircraft are plotted in Figure 10. These species have strong anthropogenic sources and a lifetime long enough to be present in remote air. Some degree of overall variability in the measured mixing ratios was observed, which is expected to be inversely related to the lifetime of each gas. Additional variability is explained by proximity to or influence by emission sources. Benzene, ethyne,, and C_2Cl_4, the most variable compounds among the ones discussed here, are the shortest lived compounds with lifetimes of approximately 1, 2, and 6 weeks respectively compared to about 14 years for HFC-134a. However, even when the overall variability is considered, we observed mixing ratios that were considerably enhanced with respect to the majority of the samples. Ethyne and benzene are good tracers of general combustion, and in many samples the ethyne mixing ratio was more than double the average that was calculated for all samples collected. Tetrachloroethylene (C_2Cl_4) and HFC-134a are usually associated with urban emissions.

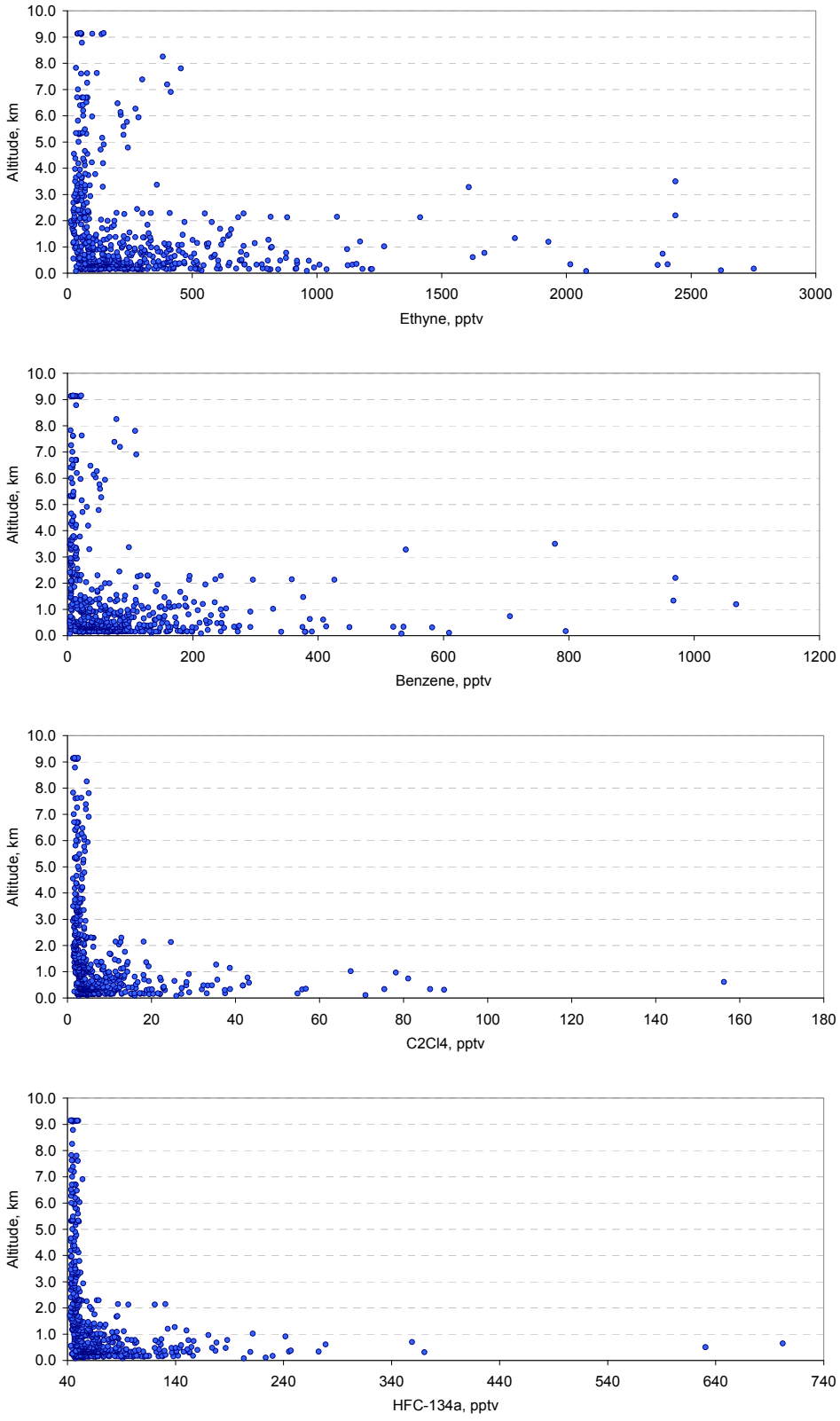

Figure 10. Altitudinal profile of the mixing ratio measured for selected VOCs.

The statistics of the samples collected during the fours ARCTAS-CARB flights are summarized in Table 2 for the 0-2 km altitudinal band to illustrate the composition of the boundary layer / low tropospheric region.

Table 2. Statistics of the samples collected below 2 km of altitude. SD = standard deviation.

	0-2 km altitude (n = 471)				
Unitis ; pptv	Minimum	Maximum	Average	1-σ SD	Median
OCS	480	707	567	37	559
DMS	LOD	204	15	30	5
CFC-12	522	654	539	10	538
CFC-11	239	498	253	18	250
CFC-113	75.0	87.4	77.8	1.1	77.7
CFC-114	15.6	17.4	16.3	0.3	16.3
H-1211	4.12	9.07	4.48	0.38	4.38
H-2402	0.49	0.54	0.51	0.01	0.52
H-1301	2.90	4.30	3.35	0.16	3.30
HCFC-22	188	926	256	84	227
HCFC-142b	18.5	856	32.6	63.1	21.9
HCFC-141b	18.1	237	26.3	14.5	22.7
HFC-134a	42.2	702	77.0	56.7	59.9
HFC-152a	5.7	398	32.9	44.1	18.1
CHCl3	5.5	56.0	13.6	6.7	11.4
CH3CCl3	11.8	17.9	12.7	0.7	12.5
CCl4	90	109	93	1	93
CH2Cl2	22.1	319	53.6	37.6	41.0
C2HCl3	0.09	300	2.56	14.38	0.75
C2Cl4	1.4	156	9.5	13.8	4.7
CH3Cl	525	1372	623	51	619
CH3Br	7.98	185	13.74	12.44	10.70
CH3I	0.019	6.331	0.731	0.723	0.515
CH2Br2	0.73	4.68	1.11	0.39	0.93
CHBrCl2	0.13	6.25	0.59	0.70	0.33
CHBr2Cl	0.04	4.43	0.39	0.51	0.19
CHBr3	0.14	8.04	1.43	1.49	0.63
Ethylchloride	0.96	13.76	2.76	1.32	2.48
1,2-Dichloroethane	5.14	33.6	11.27	2.64	10.92
MeONO2	3.68	35.8	11.09	5.25	9.41
EtONO2	1.57	37.0	9.21	5.92	7.73
i-PrONO2	0.79	89.3	13.73	13.45	9.73
n-PrONO2	0.05	8.80	1.52	1.36	1.17
2-BuONO2	0.18	90.8	11.37	14.03	6.49
3-PeONO2	0.04	18.1	2.46	2.87	1.52
2-PeONO2	0.03	33.8	4.27	5.27	2.58
3-Me-2-BuONO2	0.01	41.9	4.63	5.73	2.75
Ethane	251	24214	1460	1631	1008

Propane	14	17584	947	1691	450
i-Butane	LOD	6851	211	526	56
n-Butane	LOD	6577	271	583	95
i-Pentane	4	5451	290	519	115
n-Pentane	LOD	2555	130	244	52
n-Hexane	4	970	47	90	18
n-Heptane	LOD	391	26	38	13
2+3-Methylpentane	4	2680	133	249	49
2,3-Dimethylbutane	LOD	436	30	46	13
Propene	LOD	1910	59	162	16
1-Butene	LOD	242	32	46	18
i-Butene	LOD	223	13	22	6
trans-2-Butene	LOD	78	11	16	5
Cis-2-Butene	LOD	74	11	16	6
1,3-Butadiene	LOD	93	21	23	11
Isoprene	LOD	8130	238	854	53
Ethene	LOD	4171	267	539	107
Ethyne	15	2752	321	381	199
Propyne	LOD	99	27	23	18
Benzene	4	1067	97	119	60
Toluene	LOD	2448	129	244	48
Ethylbenzene	LOD	518	31	57	11
m+p-Xylene	LOD	1373	57	137	13
o-Xylene	LOD	394	28	49	9
n-Propylbenzene	LOD	54	10	10	7
3-Ethyltoluene	LOD	159	20	26	10
4-Ethyltoluene	LOD	74	13	13	10
2-Ethyltoluene	LOD	51	11	10	8
1,3,5-Trimethylbenzene	LOD	34	9	8	7
1,2,4-Trimethylbenzene	LOD	217	25	38	10
1,2,3-Trimethylbenzene	LOD	53	12	11	9
alpha Pinene	LOD	80	12	14	7
beta Pinene	LOD	98	7	9	5
Furan	11	246	80	80	49
Methanol	664	19264	4849	3164	4047
Ethanol	40	5407	881	901	542
Acetone	429	9391	2097	1232	1845
MEK	17	770	109	91	87
MAC	5	1063	51	98	20
MVK	5	1693	72	149	28
MTBE	1	203	8	20	2

Note: LOD for DMS is 1 pptv while that for NMHCs is 3 pptv.

In an effort to highlight differences in the VOC sources for the different source regions in the investigated area, we segregated the samples collected during the four CARB flights and the two transits (Flight 16 and Flight 24) in four main groups: samples collected over the SCAB region and specifically over the LA area, over the SJV, over San Diego, and over the border between Mexico and the U.S. Figures 11-a through 11-d illustrate the position of the samples collected within these different regions.

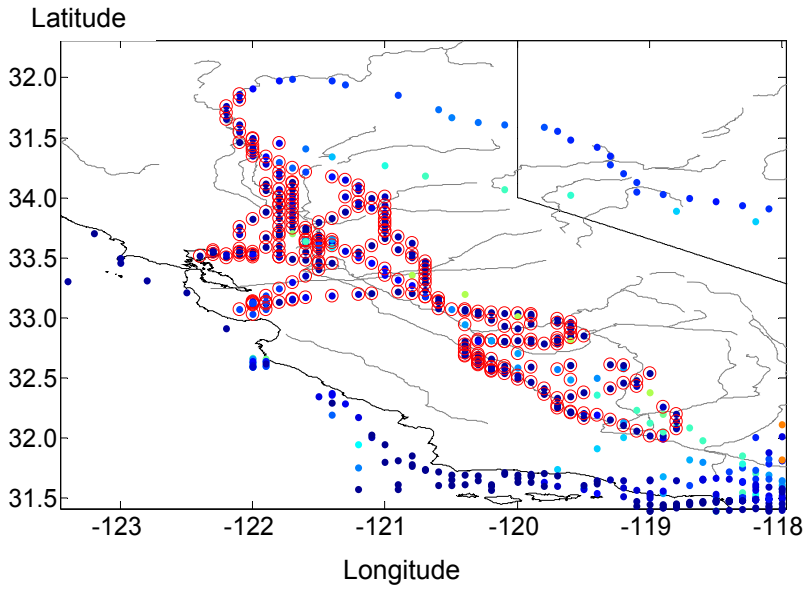

Figure 11-a. Geographical location of the samples collected over the SJV.

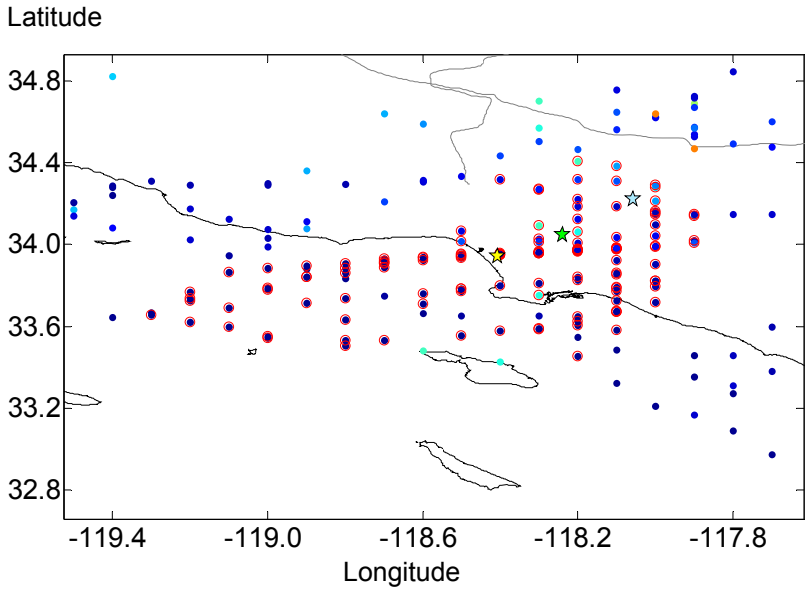

Figure 11-b. Geographical location of the samples collected over the LA area.

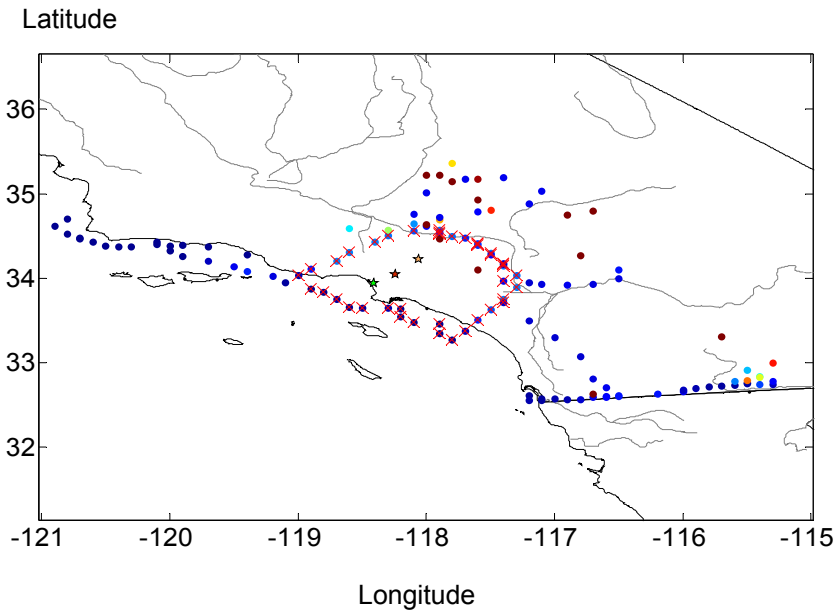

Figure 11-c. Geographical position of the samples used to represent the SCAB region.

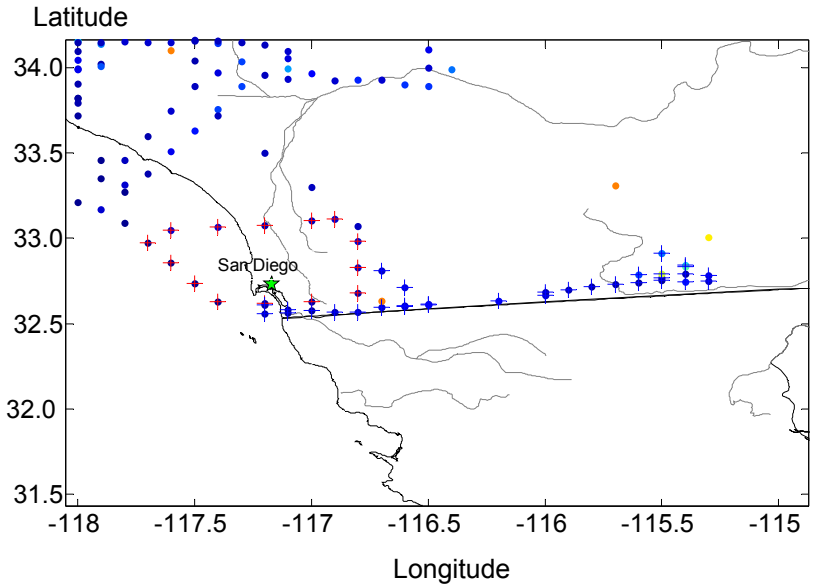

Figure 11-d. Geographical position of the samples collected over the San Diego area (red “plus”) and over the border between Mexico and the U.S (blue “plus”).

5.2 CFC replacement compounds

We present here the distribution of the halocarbon fraction measured over California focusing on CFC replacement compounds in response to one of the main objective of the ARCTAS-CARB mission (i.e. provide observations to improve emission inventories for greenhouse gases).

HCFCs and HFCs have been introduced as substitute of CFC compounds in response to the regulations imposed by the Montreal Protocol and subsequent amendments. While HCFCs still contribute to the destruction of the stratospheric ozone layer, the chlorine-free compound HFCs do not pose any treat to the ozone layer. However, because of their ability to absorb infrared radiation, HFCs are important greenhouse gases enhancing radiative forcing.

Figures 12-15 show the mixing ratios measured for the samples collected during the four ARCTAS-CARB flights and the two transits (flights 16 and 24) over the source regions previously presented.

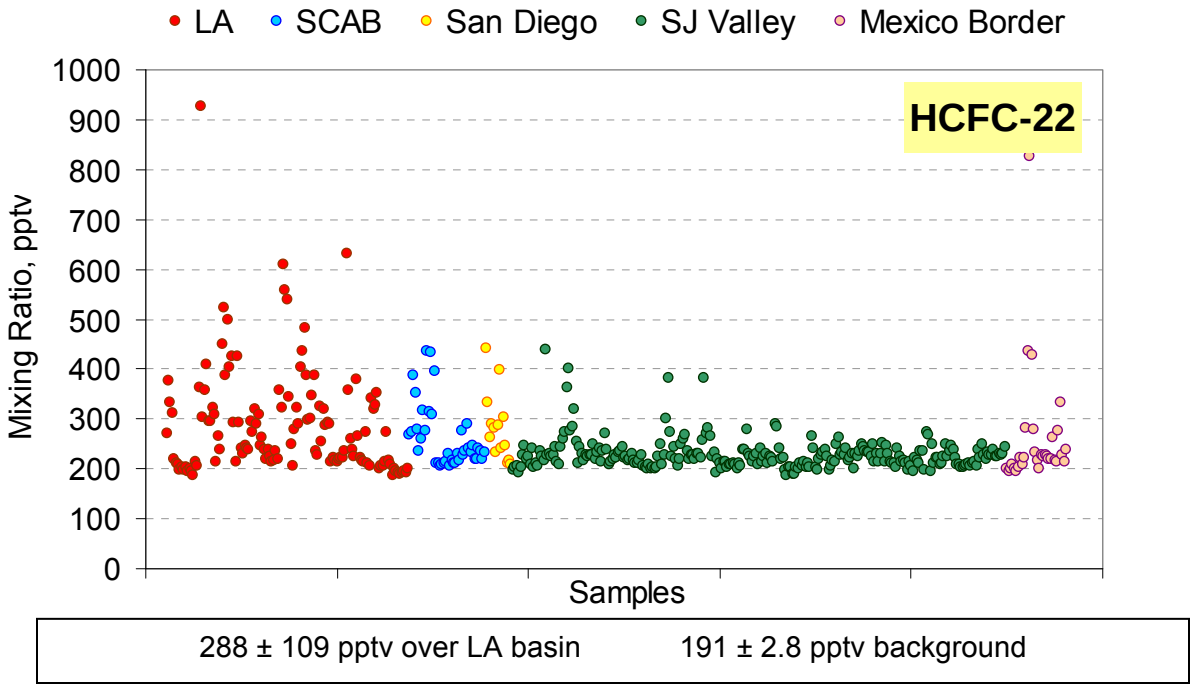

Figure 12. HCFC-22 mixing ratios.

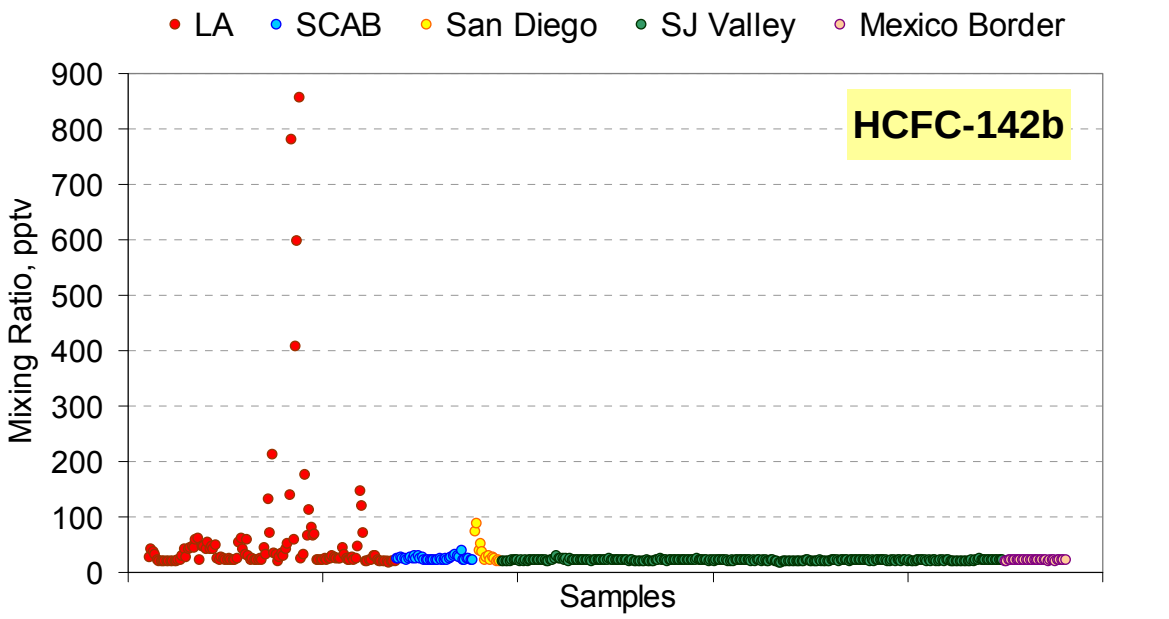

58 ± 118 pptv over LA basin	19.0 ± 0.4 pptv background

Figure 13. HCFC-142b mixing ratios

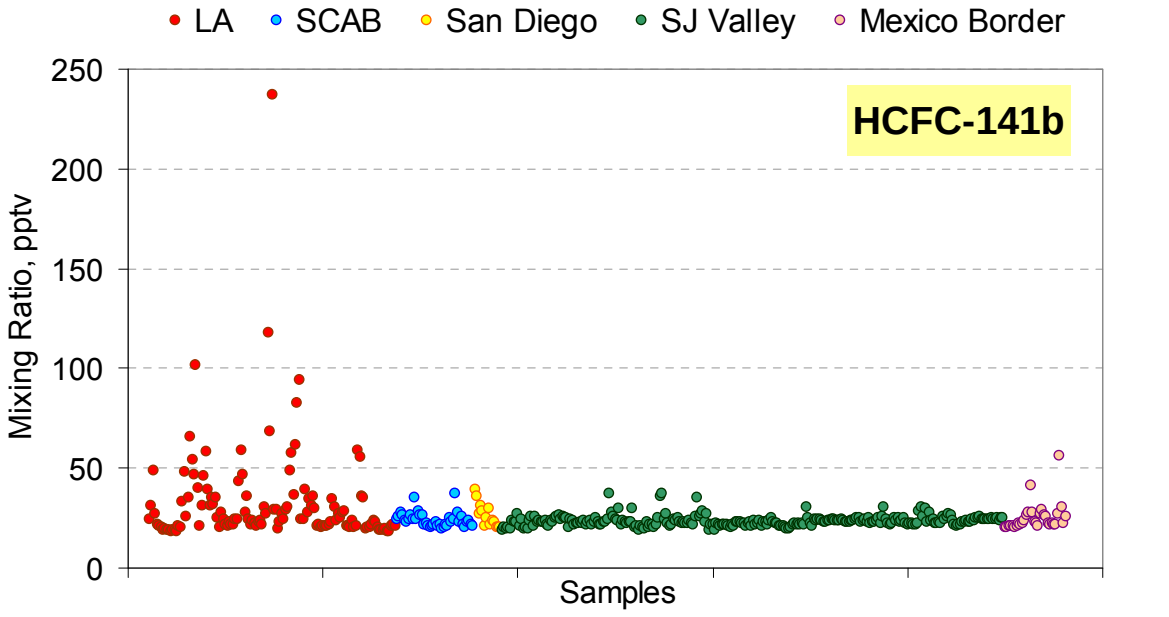

33 ± 25 pptv over LA basin	19.5 ± 0.4 pptv background

Figure 14. HCFC-141b mixing ratios

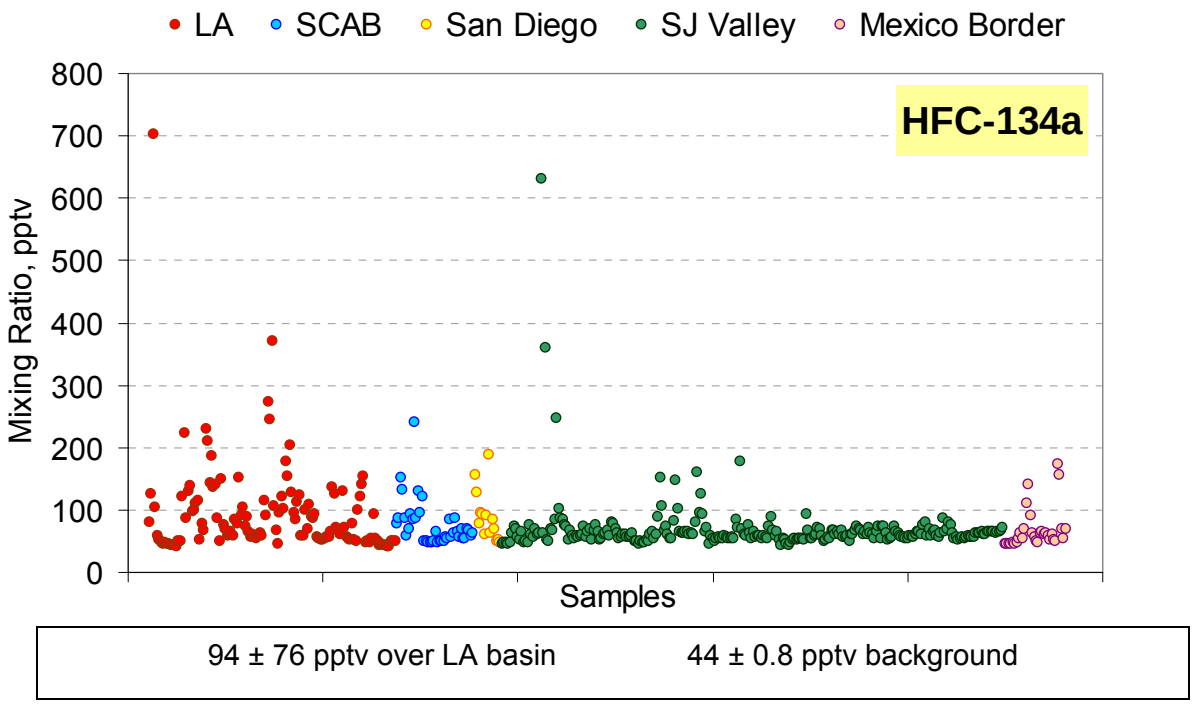

Figure 15. HFC-134a mixing ratios.

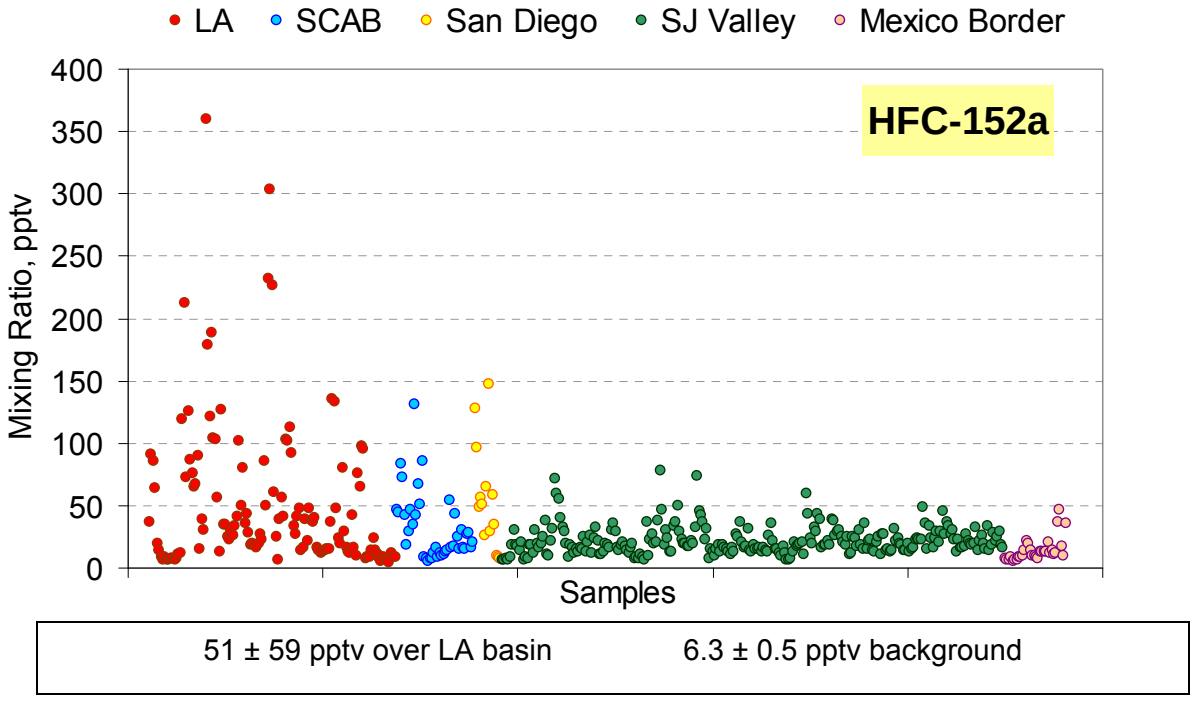

Figure 16. HFC-152a mixing ratios.

The trends illustrated in Figures 12-16 strongly suggest the presence of a significant emission source of these gases over the LA area. Specifically, high enhancements in the atmospheric levels of all the CFC replacements were measured over this source region.

The average levels (± 1-sigma SD) calculated over LA are summarized under each plot and compared to the regional background calculated as the average of the lowest quartile of the remaining ARCTAS-CARB samples collected below 8 km of altitude (to avoid clean air from stratospheric intrusions).

5.3 HFC-152a emission estimates.

The highest increase with respect to the background was observed for HCF-152a with an average mixing ratio about 10 times higher.

HFC-152a levels have been exponentially increasing in the atmosphere in the past decade (particularly in the northern hemisphere; Table 3) with the highest emissions sources located in North America.

Table 3. HFC-152a emissions from different locations – literature data

Year	Location	Emissions (Gg/yr)
1995-98	Europe	0.46 [(a)]
2000-01	Europe	0.8 [(a)]
2003	Europe	2 [(a)]
2003-04	Europe	1.5 - 4.0 [(a)]
2006	North America	16 [(b)]
2006	U.S.	12 [(b)]
2004	Australia	0.005 – 0.01 [(a)]
Late 1990s	Global	4 [(a)]
2002-03	Global	20 - 22 [(a)]
2004	Global	28 [(a)]
2006	Global	37 [(b)]

[(a)] Greally *et* al., 2007.
[(b)] Stohl *et* al., 2009.

Figure 17 shows the geographical location of the samples collected over the LA basin color coded by HFC-152a levels. Particularly high mixing ratios were observed

south-east of downtown. Some of the samples collected offshore were also characterized by elevated HFC-152a levels.

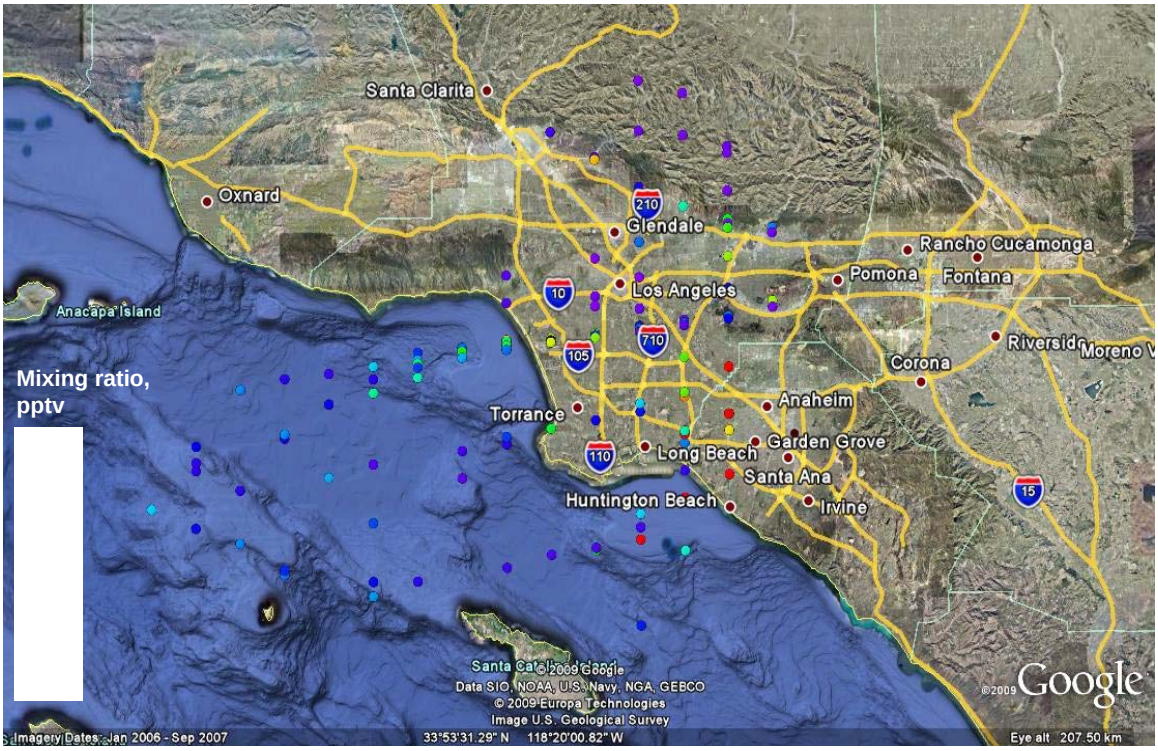

Figure 17. Mixing ratio of HFC-152a measured over the LA area during the ARCTAS-CARB flights.

In an effort to extrapolate the HFC-152a emissions from the LA basin we multiplied the HFC-152a/CO mass ratio (Figure 18) by the CO annual emission from the LA county reported by CARB (1958 tons per day – 2 x 10^9 grams per day [3]).

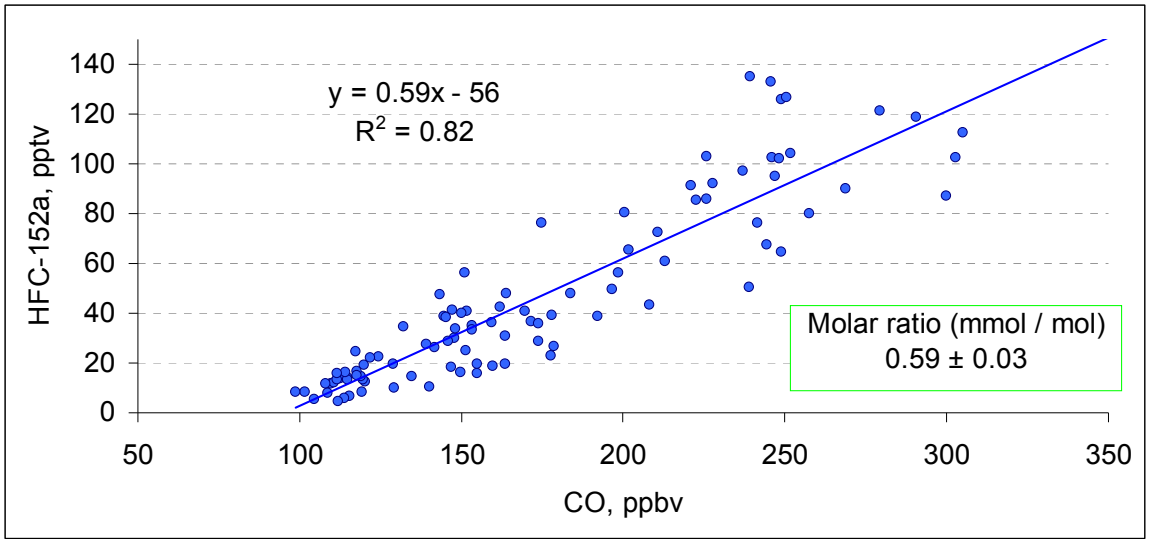

Figure 18. Plot of HFC-152a versus CO for the samples observed over the LA area.

To obtain the mass ratio, the HFC-152a/CO volume ratio (pptv/ppbv or mmol/mol) was multiplied by the respective molecular weights:

$0.59 \cdot 10^{-3}$ $(mol_{HFC152a}/mol_{CO})$ × 66 $(g/mol)_{HFC\text{-}152a}$ / 28 $(g/mol)_{CO}$ × $2 \cdot 10^{9}$ $(g/day)_{CO}$ × 365 days/yr = **1.0 Gg/yr**

According to the above calculation, we extrapolate a HFC-152a emission of 1.0 Gg/yr from the LA county. One way to estimate total emissions of HFC-152a is to use population data for LA and the US.

$$\frac{1.0\ Gg/yr\ _{(LA\ county)}}{9.9 \cdot 10^{6}\ (population\ in\ LA\ county)} \times 304 \cdot 10^{6}\ (U.S.\ population) =$$

= **31 Gg/yr (U.S.) =** U.S. estimate for 2008

According to Greally *et* al. (2007) [1], HFC-152a global emissions for the 1994-2004 period increased at a rate of about 14% per year. This increase gives a global estimate of about 45 Gg/yr for 2008. The 31 Gg/yr extrapolated for the U.S. using the ARCTAS-CARB data represents ~ 68% of the global emissions.

Air quality simulations were performed using the UCI-CIT Air Quality Model, which is a three-dimensional Eulerian urban photochemical model designed to study the dynamics of pollutant transformation and transport in the SCAB. The UCI-CIT model uses a horizontal 80x30 rectangular grid with 5 vertical layers. Each grid cell corresponds to a 5km x 5km region extending 1100m in height. The model includes the CalTech Atmospheric Chemistry Mechanism (Griffin et al., 2002a; 2002b) which consists of 445 gas-phase chemical reactions and 137 gas-phase species. The temperature, wind fields, and other meteorological parameters are taken from the September 8-9, 1993 field campaign described in Griffin et al. (2002b). In the simulations, HFC-152a is emitted from urban areas at a constant rate of 1.2×10^{-5} g m^{-2} hr^{-1} between 6 am and 10 pm. Although HFC-152a may react with OH at a rate of 3.5×10^{-14} cm^3 $molec^{-1}$ s^{-1} (at 298 K), loss due to chemical reaction is insignificant compared to loss from transport. The UCI-CIT model is run for five simulation days allowing the system to reach a steady diurnal cycle of HFC-152a. The data presented here is from the final simulation day. Figure 19 shows a contour plot of the concentration of HFC-152a in the entire SCAB at noon.

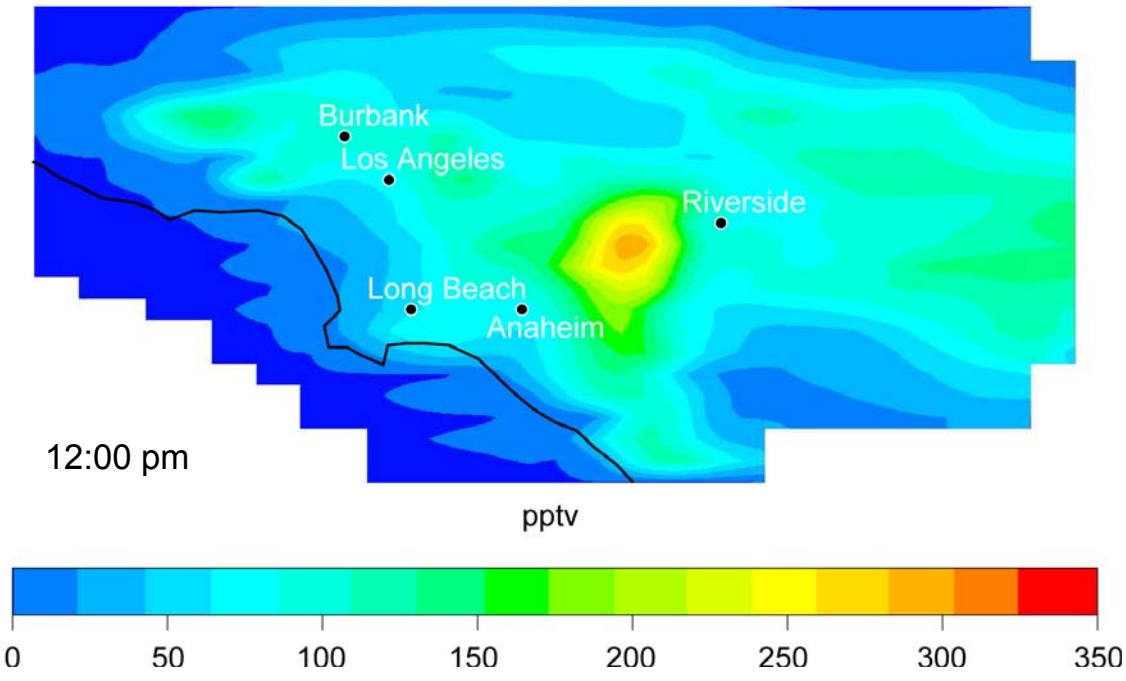

Figure 19. HFC-152a levels in the SCAB at noon.

The mixing ratios measured during the ARCTAS-CARB flights over the LA area (i.e. about 50 pptv average) are correctly predicted by the model and the emissions of 1.2×10^{-5} g m^{-2} hr^{-1} used in the simulation agree very well with the emission extrapolated from the HFC-152a/CO slope (~ 1.1 Gg/yr vs 1.0 Gg/yr).

6. Oxygenated compounds

6.1 Airborne data used in Dairy Emissions Analysis

The data used in this section were obtained during a total of seven flights including two test flights and five science flights. Test flights were conducted in order to provide all researchers aboard the NASA DC-8 aircraft an opportunity to not only calibrate their instruments but to also ensure that the instruments were operating at optimum capacity. Out of the remaining five science flights, four of them were flights which were a part of the ARCTAS-CARB study, while the final research flight consisted of a low-level segment through the San Joaquin valley as part of the transit back into California from Cold Lake, Canada (i.e. Flight 24).

The four flights that engaged in low-level runs through the valley were test flights (TF) 1 and 2, science flight (SF) 13 and transit flight (TF) 24. A summary of the flights and their durations is presented in table 4.

Table 4: Summary of flights that were analyzed for emissions from dairy farms.

Flight	Date	Duration	Hours of flight (PST)	Ave. Temp in SJV (°C)
TF 1	3/18/08	3 hrs 35 mins	11.05 am to 2.40 pm	20
TF 2	3/20/08	4 hrs 8 mins	11.07 am to 3.15 pm	18
SF 13	6/20/08	7 hrs 48 mins	10.32 am to 6.15 pm	38
TF 24	7/13/08	5 hrs 50 mins	10.57 am to 3.47 pm	35

With the exception of selected atmospheric source tracers, fewer compounds were analyzed on the test flights compared to the science flights as most of the instruments on the plane were not involved in data collection but in the process of instrumental calibration. The data presented for both test flights primarily consists of data (whole air) collected by the UCI team.

6.2 Effects of California Wild fires on airborne data

Every year California faces the threat of fire season. The emissions from biomass burning not only affect the air quality on the ground, but also extend up into the free troposphere. Evidence of biomass burning is seen in the data through the quantification of specific biomass burning tracers. These include CO, CH_4 and CH_3Cl. During all four ARCTAS-CARB flights, evidence of wild fires burning in California can be observed. By the month of June, the wild fires had been burning for approximately three months causing the SJV to be inundated with smoke. For flights 13 and 24, we are unable to distinguish between the biomass burning emission sources of the air masses observed at 1000 ft in altitude and other individual emission sources in the SJV. The extent to which the biomass burning emissions have consumed the SJV air basin is shown in figure 20.

Figure 20. MODIS image of California taken on June 20th, 2008, with major cities and significant wild fires highlighted in the image (UMBC, 2008).

Photochemical reactions of the compounds emitted from biomass burning must also be considered as many short-lived gaseous species react in the atmosphere to form secondary products. For example, one of the compounds given off by biomass burning is formaldehyde (CH_2O). In the atmosphere, CH_2O is able to photodissociate to produce

carbon monoxide (CO) and the very reactive perhydroxyl (HO_2) radical, as shown in the reaction below (Holzinger *et* al., 1999):

$$CH_2O + h\nu\ (+2O_2) \rightarrow CO + 2HO_2 \qquad (9)$$

This HO_2 radical can then react with several other species in the atmosphere. The CO produced in this reaction may also interfere with our measurement of CO, as an urban tracer.

An important biomass burning tracer used in this study is methyl chloride (CH_3Cl; with an average background level in the atmosphere of about 550 pptv). All the flights showed elevated levels of CH_3Cl 1000 ft above the valley floor.

Since the fire season didn't begin till March 2008, and both test flights 1 and 2 occurred at the beginning of the flare up, the effect of biomass burning on the overall data is still minimal and distinguishable from other emission sources. By examining the two main biomass burning tracers, CH_4 and CH_3Cl, we are able to distinguish between biomass burning plumes and all other sources (dairy and urban/industrial sources). By plotting biomass burning tracers against each other, and measuring their correlations, we are able to isolate biomass burning plumes within the air mass sampled. Figure 21 shows CH_4 versus CH_3Cl, with the different plumes highlighted in different colors.

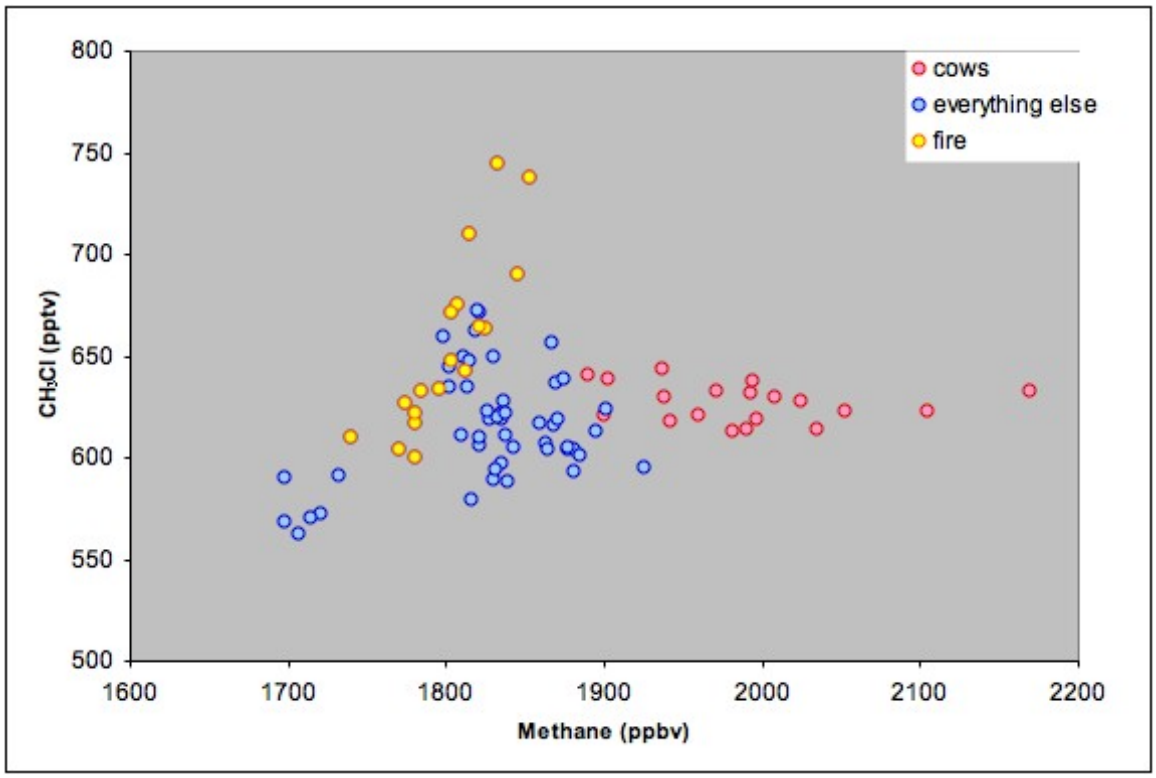

Figure 21. Test flight 2: Analysis of the data collected over the entire flight in search for emissions originating from biomass burning sources.

Within the biomass burning plume, as highlighted by the yellow points in figure 21, both CH_4 and CH_3Cl are well correlated with a coefficient of determination (R^2) value of 0.73. However, within the hypothesized dairy plume, as indicated by the pink points in figure 21, there is no correlation (R^2 value of 0.04). Similarly, the remaining air masses analyzed for test flight 2 (blue points in figure 21) show a poor correlation between CH_4 and CH_3Cl with a R^2 value of 0.1. Based on the correlations alone, we can conclude that a portion of air mass sampled in test flight 2 had a biomass burning source, and that not all of the methane present in the SJV is a product of dairy farming. Figure 21 illustrates the importance of using tracers in order to analyze emission sources in the atmosphere.

6.3 Significance of "urban" tracers

To differentiate between different emission sources it is important to isolate urban emissions from dairy farm emissions. This is especially important for key compounds such as methanol and acetone which may have more than one contributing source in the SJV. The two VOCs commonly used to distinguish urban air masses are CO and ethyne

(C_2H_2), which are the main exhaust components of internal combustion engines (Barletta *et* al., 2002). The photochemical lifetime of CO and C_2H_2 is about two months and three weeks respectively (Khalil *et* al., 1990; Simpson *et* al., 2004). In the airborne data set, CO was measured *in situ* on the NASA DC-8 airplane by the differential absorption CO measurement (DACOM) instrument (Sachse *et* al., 1987).

There are two industrial solvents that are also used as urban/industrial tracers - perchloroethylene (C_2Cl_4) and tetrafluoroethane (HFC-134a). The photochemical lifetime of C_2Cl_4 and HFC-134a are 3-4 months and 14 years respectively (Simpson *et* al., 2004; McCulloch *et* al., 2003). The current atmospheric mixing ratios of C_2Cl_4 and HFC-134a are 5-10 pptv and ~ 50 pptv respectively (Simpson et al., 2004; O'Doherty et *al*., 2008). All of these urban tracers have long strong anthropogenic sources and reasonably long lifetimes allowing them to be observed in remote air.

Based on the data obtained in previous flux chamber studies and the estimates of ventilation within the valley, it appears that there are other significant emission sources of ethanol within the SJV besides the silage piles on dairy farms. Based on its lifetime, we do not expect ethanol to have reacted by the time they have reached an altitude of 1,000 ft above the valley floor. In the airborne data, we are able to clearly distinguish between urban/industrial sources and dairy farm sources. In test flight 1, the presence of an urban/industrial source of ethanol is examined by plotting CO against ethanol (figure 22). Based on the graph, two distinct trends are observed, each corresponding to a specific emission source. We make the assumption that the trend with the pink points in the plot corresponds to emissions from dairy farms, while the other remaining blue points in the plot corresponds to emissions from an urban/industrial source. The correlation of CO and ethanol within the dairy plume is weak with a R^2 value of 0.31 while the same correlation within the remaining air mass is stronger with a R^2 value of 0.67. Based on the correlations, it is clear that there are two different sources of ethanol within the SJV, one with a greater urban/industrial source origin than the other. Hence, we can use the R^2 value correlations in this case in order to identify individual source emissions.

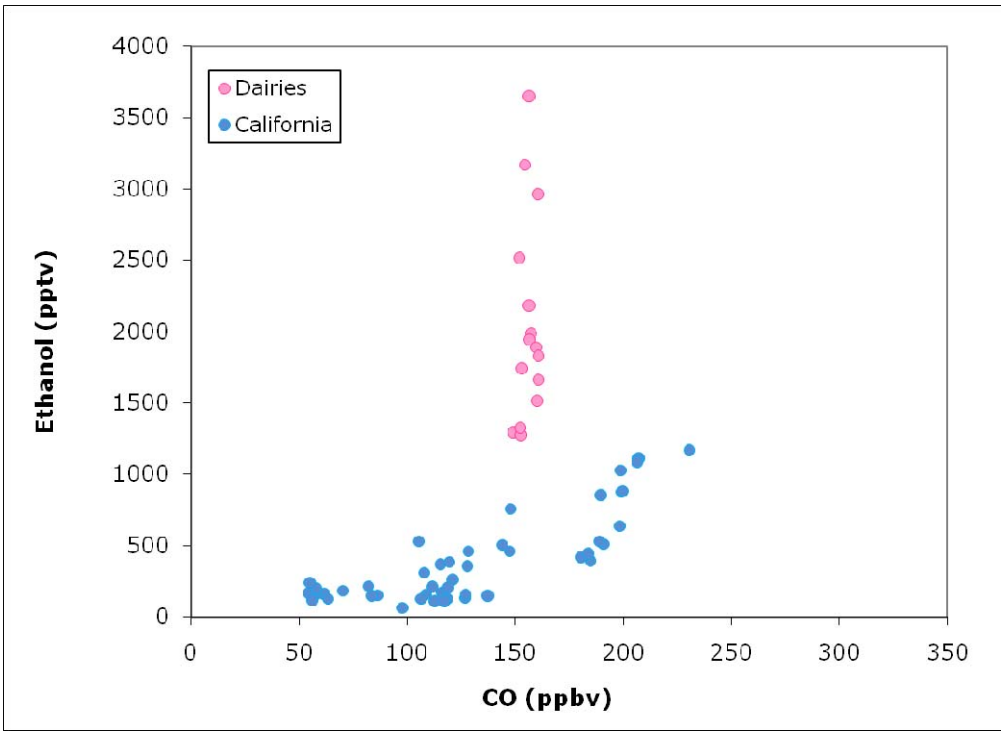

Figure 22. Test flight 1: Analysis of the data collected over the entire flight in search for emissions originating from urban/industrial sources and dairy farm sources.

Similarly, when we plot another urban/industrial tracer, C_2Cl_4 against ethanol, we have a similar graph as shown in figure 23.

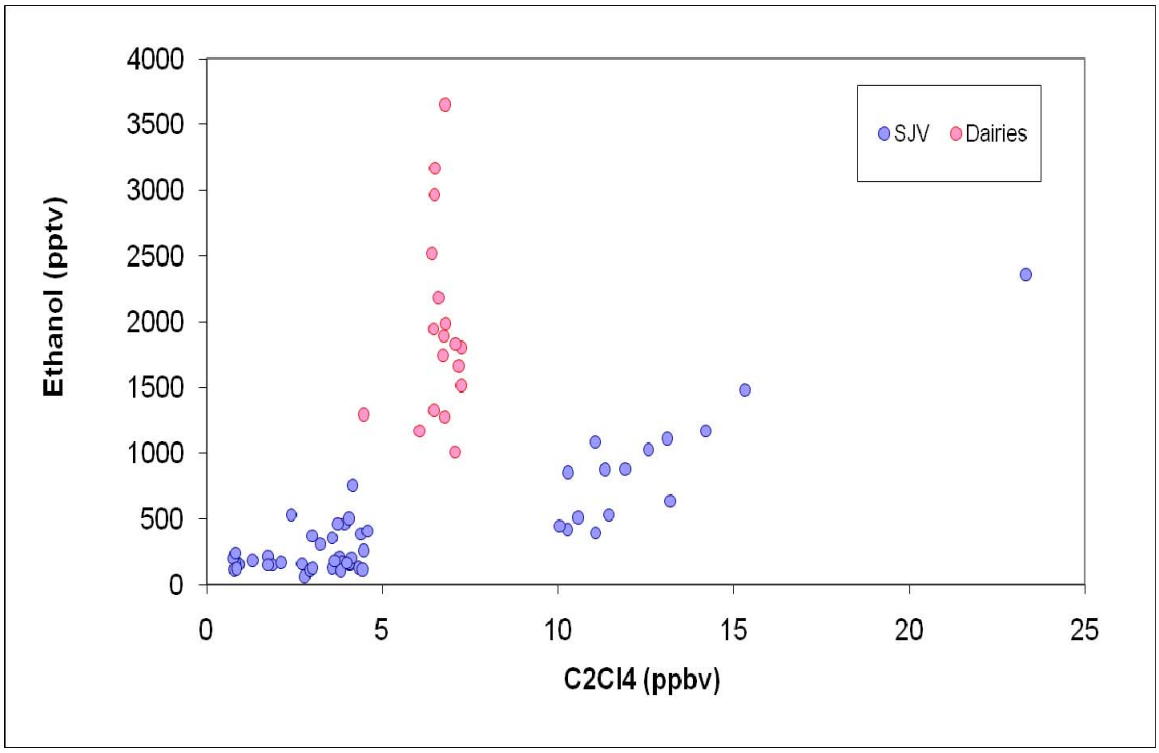

Figure 23. Test flight 1: Analysis of the data collected over the entire flight in search for emissions originating from urban/industrial sources using the tracer, C_2Cl_4.

Once again, two trends are evident in the data corresponding to two different emission sources. In figure 23, the correlation between C_2Cl_4 and ethanol in the dairy plume is lower (R^2 = 0.10) than that of all other samples taken during the flight over California (R^2 = 0.77). Similar plots are observed for test flight 2, science flight 13 and transit flight 24. We are able to identify the dairy plume based on its weak correlations with specific urban/industrial tracers as well as the enhanced levels of ethanol observed with relative constant level of urban/industrial tracers within the plume. This would not be the same in the case of an urban/industrial plume, in which both compounds would be elevated. We can further illustrate this point by plotting the two urban/industrial tracers against one another. Figure 24 is a plot of CO against C_2Cl_4 mixing ratios observed in test flight 1.

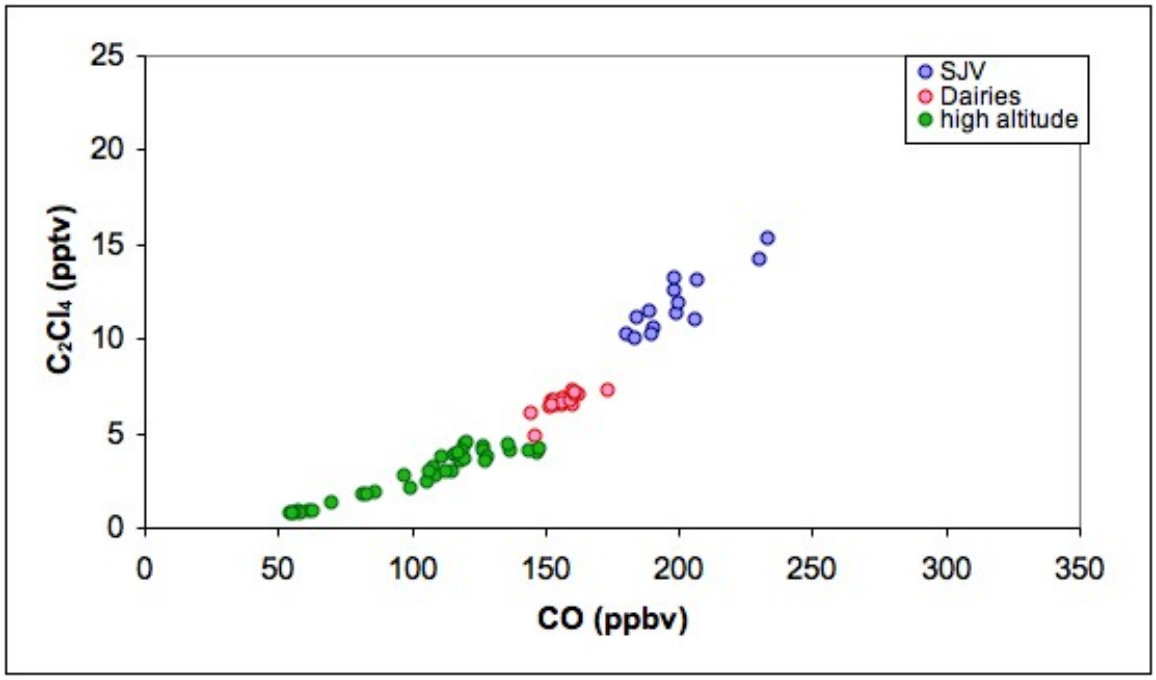

Figure 24. Test flight 1: Analysis of the data collected over the entire flight. The plot of CO against C_2Cl_4 is color-coded showing the separation of sources within the air mass sampled in the flight above California.

Figure 24 is color-coded showing the separation of the air mass measured during the flight into different sources. As observed in figure 22, in the dairy plume, the CO mixing ratio did not exceed 174 ppbv, while the C_2Cl_4 mixing ratio did not exceed 7.3 pptv. The lower values of CO (< 150 ppbv) and C_2Cl_4 (< 4.5 pptv) observed in figure 24 are high altitude samples and are representative of "clean" background air.

6.4 Effects of dairy farming on air quality in the SJV

The data obtained from the airborne study allowed us to conduct a "top down" assessment of the impact selected oxygenates have on SJV air quality. Table 5 lists the average oxygenate levels found in the SJV legs of the 4 flights through California. The average of the samples collected above 20,000 ft is here considered representative of the background.

Table 5. Summary of the average mixing ratios observed for four oxygenates and methane during the four flights over the SJV. Units: ppbv.

Sampling location	Ethanol	Methanol	Acetaldehyde	Methane
Background average (> 20,000 ft)	0.55	0.54	0.24	1800
Test flight 1 average (1,000 ft)	2.0	4.7	0.9	2040
Test flight 2 average (1,000 ft)	2.4	3.9	0.7	2010
Flight 13 average (1,000 ft)	2.3	5.8	0.9	1980
Flight 24 average (1,500 ft)	2.4	6.3	1.3	1930

In order to determine if any trends are present in the emissions of each oxygenate, emission ratios are used. Based on the ethanol and methanol mixing ratios presented in Table 5, we can determine the average ethanol to methanol (C_2H_5OH/CH_3OH) ratio for each flight. The C_2H_5OH/CH_3OH ratios for test flights 1 and 2, science flights 13 and 14 are 0.43, 0.62, 0.39 and 0.38 respectively versus a C_2H_5OH/CH_3OH average ratio of 1.03 in the background. This suggests that by the time ethanol and methanol reach the troposphere, the ratio of one to the other is approximately 1. The lower ratios observed during the flights (especially flights 13 and 14) suggest the presence of elevated methanol levels compared to ethanol levels. There are several possible explanations for this which will be discussed in the next section.

6.5 Alternate sources of methanol in the SJV

Looking at the airborne data, methanol levels at the surface are elevated significantly above background, suggesting the presence of an additional methanol source in the SJV. Other sources of methanol besides biomass burning may also be present in the valley, however, at this point in our research, we are unable to determine if and what they might be. Similarly, the same argument for elevated methanol levels can be applied to flights 13 and 24. As mentioned earlier, by this point in the fire season, the emissions from the wild fires had permeated throughout the valley, resulting in a well mixed layer trapped in the SJV. As the emission source of methanol had been fairly strong and consistent for months, by the months of June and July, the average methanol level observed throughout the valley was uniformly elevated as compared to background levels. Exceptions to this were active large wild fires, which created hot spots of elevated biomass burning emissions above the already elevated levels which were impacting the valley air basin. The emissions from the fires mask the relatively lower level emissions of

methanol from dairy farms, hence making it difficult for us to use methanol as a tracer for dairy farms in the SJV for flights 13 and 24. Figure 25 is a graph plotting methanol mixing ratios for flight 13. The hot spots of methanol observed correspond with major wild fires burning in California in the week of June 20th, 2008, as shown in figure 26. Google earth plots are used in both figures 25 and 26 in order to provide a clear comparison between the MODIS fire imagery of California and the observed methanol mixing ratios.

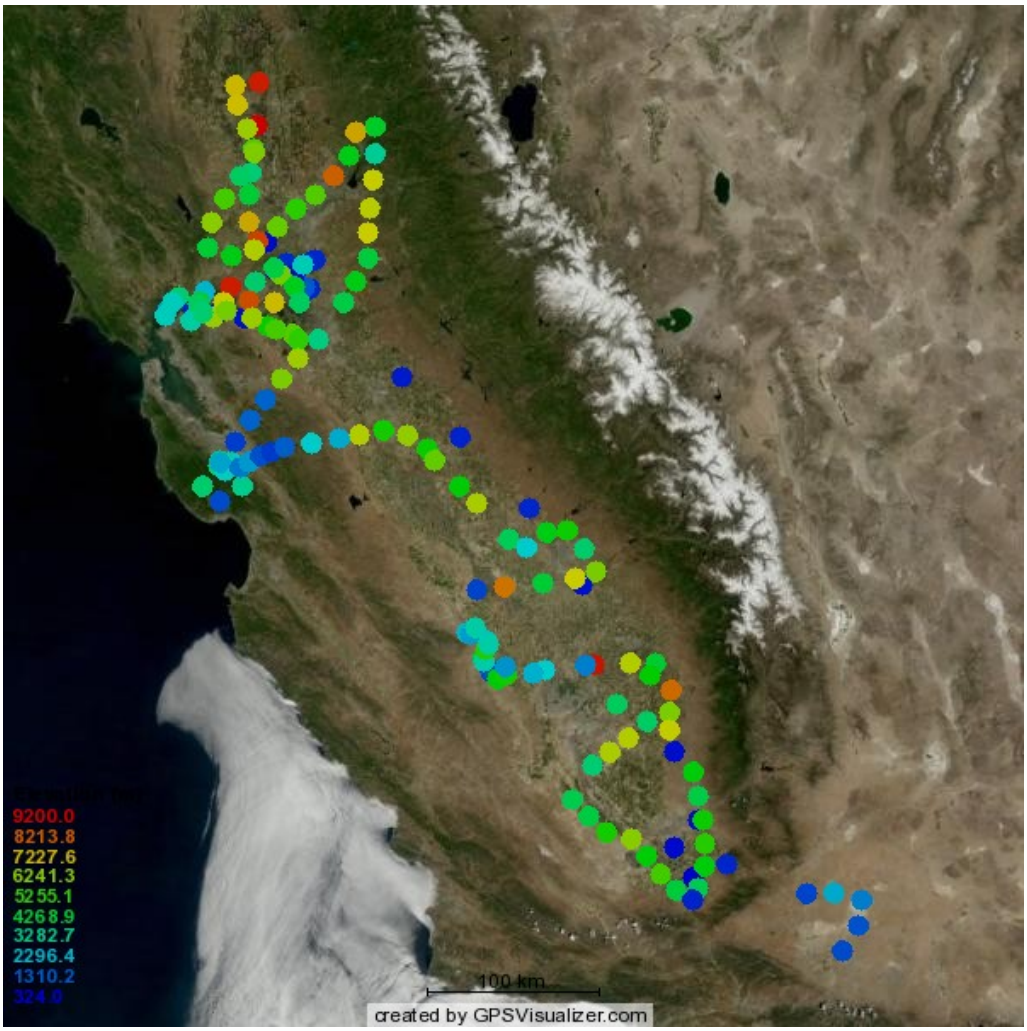

Figure 25. Google earth plot of methanol mixing ratios observed for science flight 13 through California on June 20th, 2008.

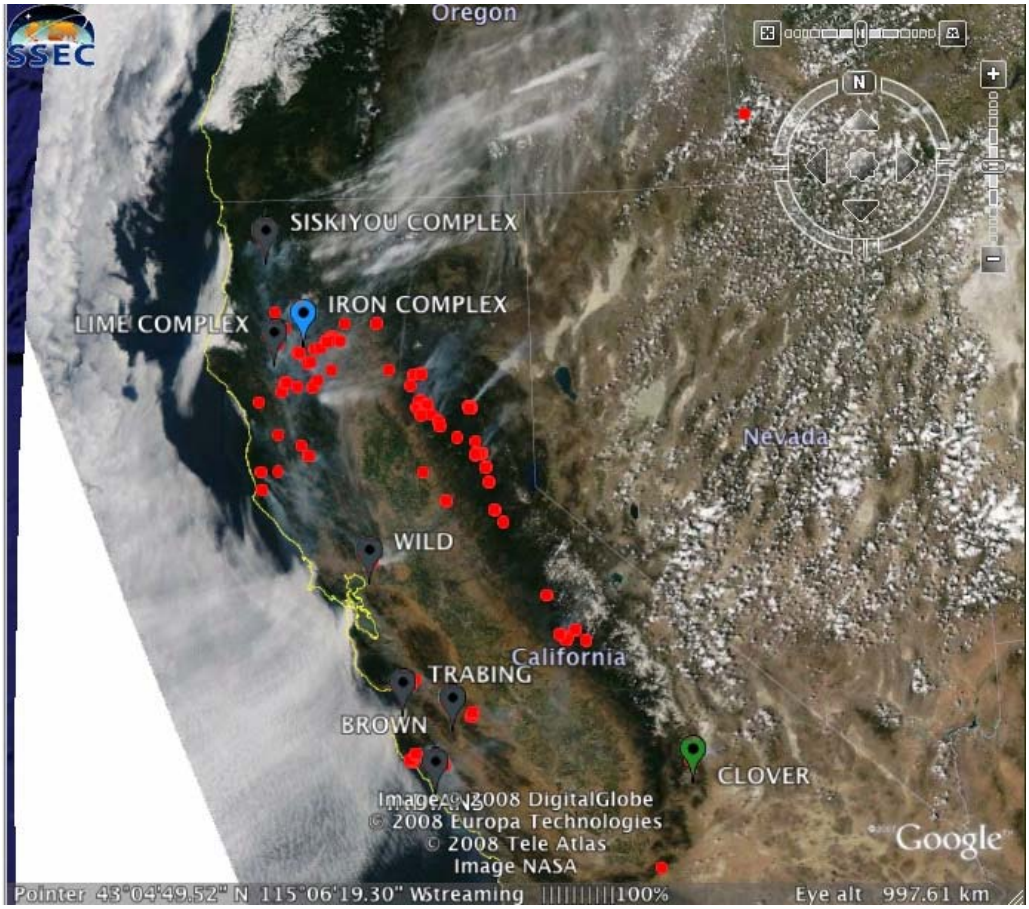

Figure 26. MODIS imagery of the California wild fires burning in the week of June 20th, 2008 (UMBC, 2008).

Due to the emissions from the wild fires, and its effects on the ethanol to methanol ratio, we are unable to use the measured methanol mixing ratios for both flights 13 and 24. All the flights showed elevated levels of acetone compared to background levels measured at 20,000 ft. Both flights 13 and 24 also show elevated levels of acetaldehyde compared to those measured in test flights 1 and 2. Just like methanol, Holzinger *et* al. (1999) report the emissions of both acetone and acetaldehyde from biomass burning. The estimated global emissions of acetone and acetaldehyde from biomass burning are determined to be (2.3 ± 1.2 to 6.1 ± 3.1) Tg and (3.8 ± 1.6 to 10 ± 4.2) Tg respectively (Holzinger *et* al., 1999). Again, due to the effects biomass burning emissions have on the average mixing ratios of the 4 oxygenates found in the valley, we are unable to use flights 13 and 24 to accurately determine the effects that dairy oxygenate emissions have on the SJV air basin. It is interesting to note though, for reasons unknown, despite methane being a well-known biomass burning tracer, the

average methane mixing ratio observed for flight 24 is lower than all of the 3 other valley flights.

6.6 Average ethanol mixing ratios observed in the SJV

The average ethanol mixing ratio observed is overall constant throughout the valley for all 4 flights. Figure 27 and 28 are plots of the ethanol mixing ratios observed in both test flights 1 and 2. The ethanol hot spots of elevated ethanol mixing ratios correspond to the nation's top three dairy producing counties, hence the counties with the most number of dairy cows.

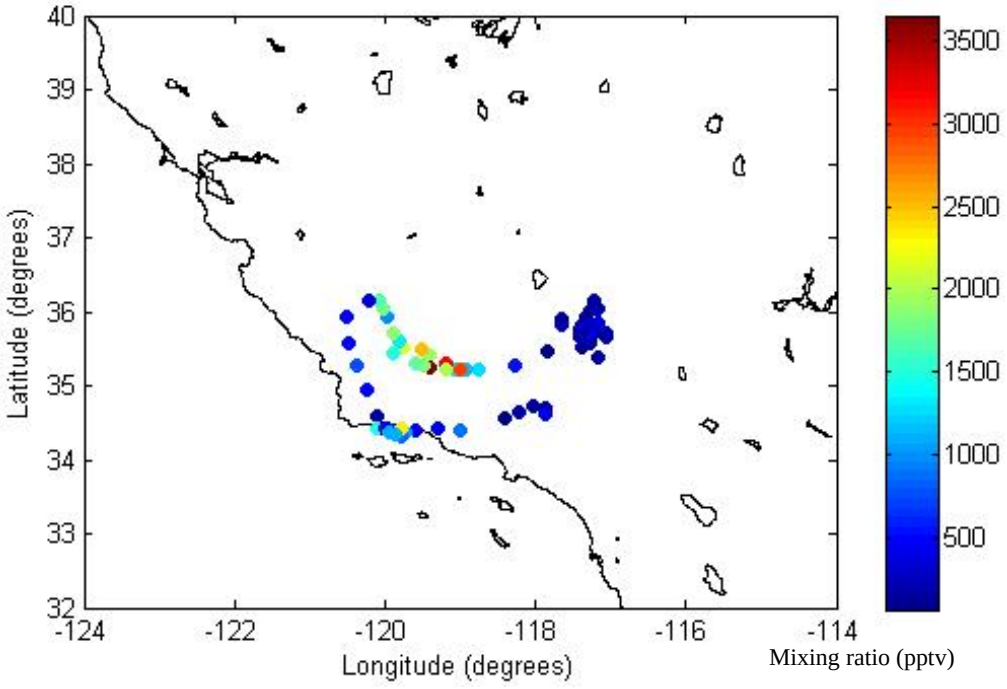

Figure 27: Test flight 1: Ethanol mixing ratios observed throughout the entire flight over the state of California.

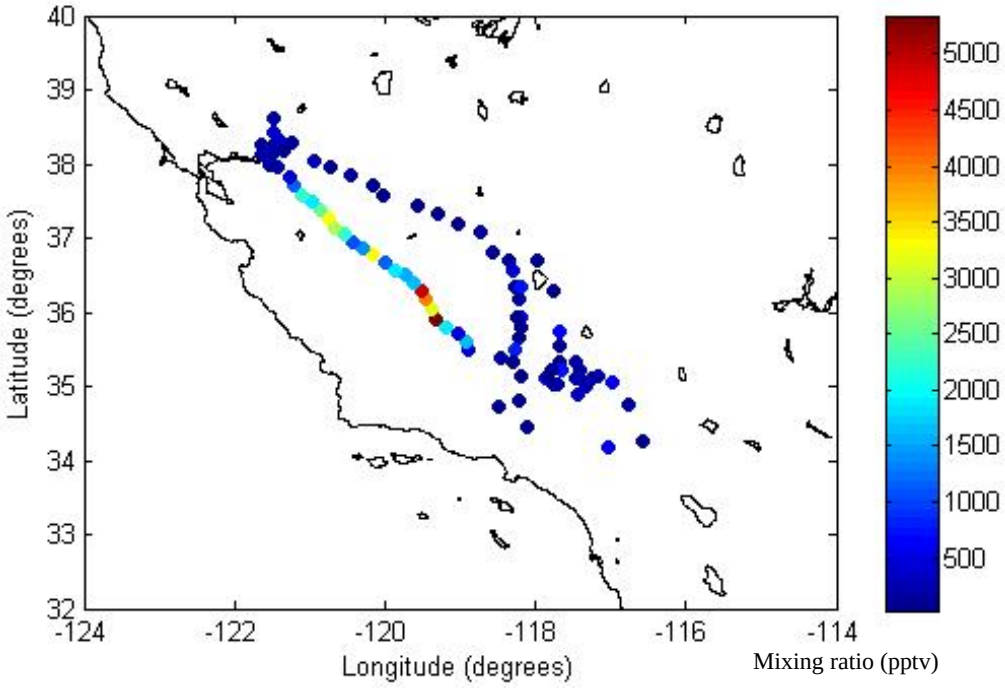

Figure 28. Test flight 2: Ethanol mixing ratios observed throughout the entire flight over the state of California.

Both test flights show elevated levels of ethanol (>1500 pptv) mainly throughout the low level leg of the flight through the SJV. If we make the assumption that all the ethanol being emitted in the valley is from dairy farms alone, and that the average ethanol mixing ratio in the valley is 2.2 ppbv at 1000 ft, with dairy farms as the source, the C_2H_5OH/CH_3OH ratio observed for test flight 1 is about 0.5. Figures 29 and 30 show similar plots for methanol mixing ratios observed in both test flights 1 and 2.

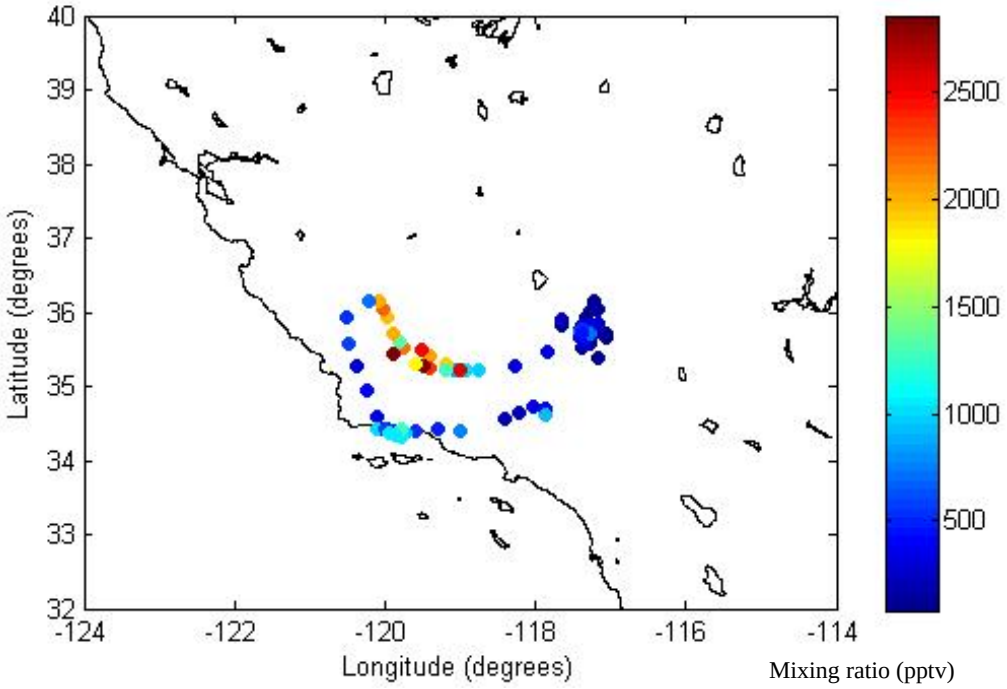

Figure 29. Test flight 1: Methanol mixing ratios observed throughout the entire flight over the state of California.

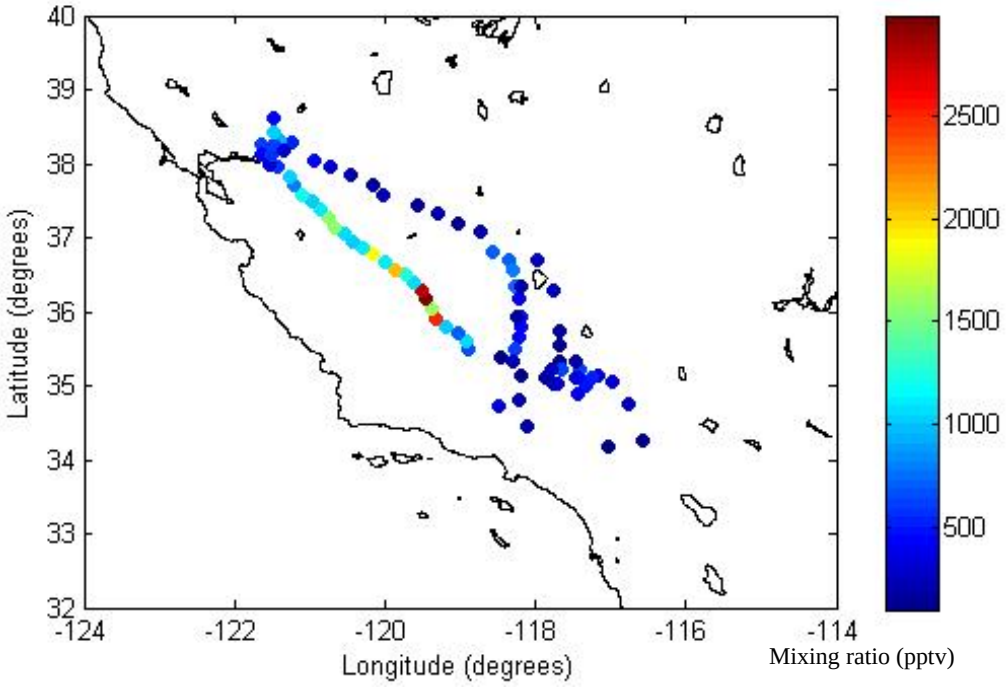

Figure 30. Test flight 2: Methanol mixing ratios observed throughout the entire flight over the state of California.

As mentioned earlier, methane can also be used as a tracer for dairy farm emissions. Despite the average methane mixing ratios reported in table 5 being only slightly higher than background, we are still able to detect elevated levels of methane through the SJV, corresponding to intense dairy farm activity. Figures 31 and 32 are plots of methane mixing ratios observed during both test flights 1 and 2.

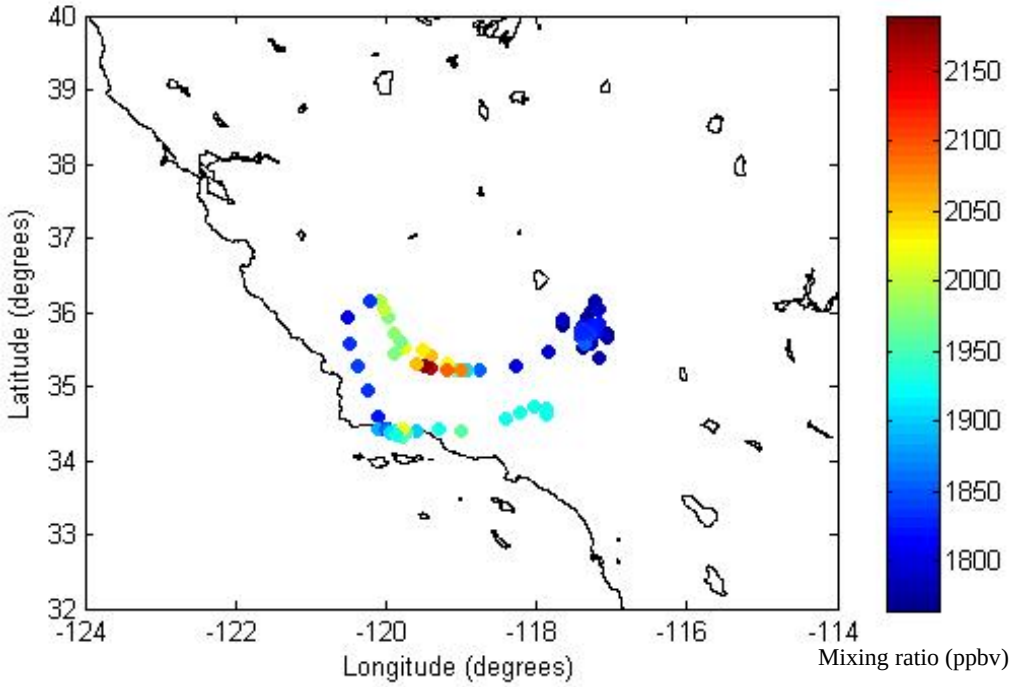

Figure 31. Test flight 1: Methane mixing ratios observed throughout the entire flight over the state of California.

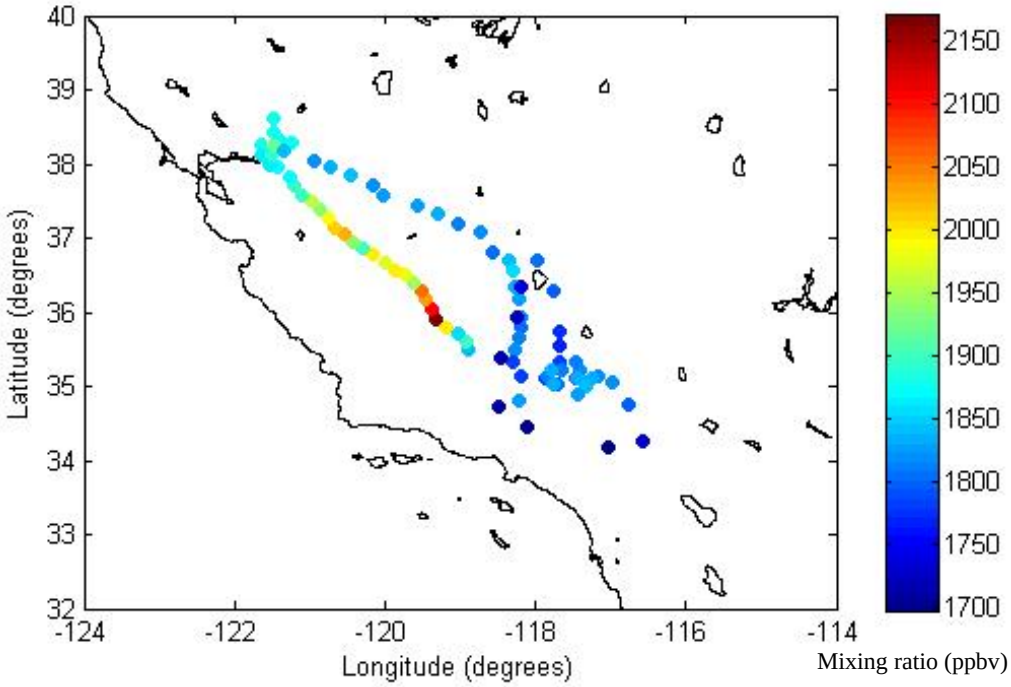

Figure 32. Test flight 2: Methane mixing ratios observed throughout the entire flight over the state of California.

7. Final report Technical Sub-Contract

To the University of California, Irvine
For submission to the California Air Resources Board

ARCTAS- California 2008: An airborne mission to investigate California air quality

Principal Investigator
Ronald C. Cohen

Professor, Department of Chemistry and
Department of Earth and Planetary Science
University of California, Berkeley
Berkeley, CA 94720-1460
(510) 642-2735
(510)643-2156 (FAX)
e-mail: rccohen@berkeley.edu

This subcontract provided support to a joint UCI, UC Berkeley, NASA proposal aimed at making observations of atmospheric composition in California in support of ARB regulatory objectives with respect to air quality and climate change. Tasks the Cohen team at Berkeley contributed to the ARCTAS-California 2008 experiments were as follows.

1) ***Integrate instrument for measurement of NO_2, total peroxynitrates, total alkyl and multifunctional nitrates and HNO_3 aboard the NASA DC-8.***
2) ***Participate in flight planning discussions using recent experience in BEARPEX and other California ground based experiments and modeling analyses as a guide.***
3) ***Complete final data from the Berkeley measurements and report to the NASA archive. Provide aid to ARB, if desired, in making the complete NASA archive of all measurements in CA as a separate data file.***
4) ***Initial observation based analyses: Although final analyses will require more time than is provided under this contract, the Berkeley group plans to focus its efforts on observation based analyses aimed at using observations to assess correlated sources of VOC and NO_x, sources of NO_x alone and the effects of NO_x on a) HO_x radicals, b) inorganic and organic aerosol production and c) production of O_3. We expect to provide initial assessment of progress in these areas during this contract and then to complete analyses and publish them with continued NASA support after the expiration of this contract.***

Tasks 1 and 3: Observations

The bulk of the effort for this subcontract was dedicated to tasks 1 and 3. The instrument was integrated into the payload as required by the schedule and final data from the mission was reported to the archive by the required deadlines. Observations were reported for all of the flights as the instrument performed flawlessly. The measurements

we made were of NO_2, total peroxynitrates (ΣPNs), and total alkyl and multifunctional nitrates (ΣANs). As there were two other HNO_3 instruments aboard the plane we did not emphasize HNO_3 measurements, instead devoting more attention to the other three chemical species. The measurements were made using the method of thermal-dissociation laser-induced fluorescence (Day et al. 2002, Thornton et al. 2000).

Briefly, observations described here were made aboard the NASA DC-8. NO_2, ΣPNs, and ΣANs were measured using the Berkeley thermal dissociation-laser induced fluorescence instrument (Day et al., 2002; Thornton et al., 2000). Briefly, gas is pulled simultaneously through three channels consisting of heated quartz tubes maintained at specific temperatures for the dissociation of each class of compounds above. Each heated section is followed by a length of PFA tubing leading to a detection cell where NO_2 is measured using laser-induced fluorescence. Due to differing X-NO_2 bond strengths, ΣPNs, ΣANs and HNO_3 all thermally dissociate to NO_2 and a companion radical at a characteristic temperature. The ambient channel measures NO_2 alone, the second channel (180˚C) measures NO_2 produced from the dissociation of ΣPNs in addition to ambient NO_2 (the observed signal is NO_2+ΣPNs) and the third channel (380˚C) measures NO_2+ΣPNs+ΣANs. Concentrations of each class of compound correspond to the difference in NO_2 signal between two channels set at adjacent temperatures. The difference in NO_2 signal between the 180˚C and the 380˚C channel, for example, is the ΣANs mixing ratio. The instrument deployed for ARCTAS had a heated inlet tip that split in two immediately. One third of the flow was immediately introduced to heated quartz tubes for detection of ΣANs while the other two-thirds was introduced to an additional heated quartz tube for detection of ∑PNs and an ambient temperature channel for detection of NO_2.

Ambient NO_2 and NO_2 produced by thermal dissociation were observed by laser-induced fluorescence as described in detail by Thornton et al. (2000). Briefly, a tunable dye laser is pumped at 7 kHz by a Q-switched, frequency doubled Nd^{+3}YAG laser. The incoming gas is cooled through the use of a supersonic expansion (Cleary et al., 2002) and the dye laser, utilizing Pyrromethene 597 in isopropanol, is tuned to an isolated rovibronic feature of jet-cooled NO_2 at 585 nm. The frequency is held for 9 seconds at the peak of this feature and then for 3 seconds at an offline position in the continuum absorption. The ratio of peak to background fluorescence of the chosen feature is 10 to 1 at 1atm and the difference between the two signals is directly proportional to the NO_2 mixing ratio. The laser light is focused in series through two multi-pass (White) cells (discussed in more detail below) and the red-shifted fluorescence is detected using a red-sensitive photomultiplier tube (Hamamatsu). Fluorescence counts are collected at 4 Hz, scattered light at wavelengths less than 700nm is rejected by band-pass filters and time-gated detection is used to eliminate noise resulting from scattered laser light in the cell. We observe a dependence of NO_2 fluorescence on the external pressure. We calibrate the NO_2 LIF vs. altitude by direct measurement of NO_2 from a standard addition during a test-flight. Calibrations were performed at least once every two hours during a level flight leg using a 4.5ppm NO_2 reference gas with a stated certainty of +/- 5%. The reference gas was compared to a library of standards in lab both before and after the campaign. The individual standards are compared on a regular basis (about every 6 months) to ensure stability and highlight when a given tank has degraded. These standards have been observed to remain stable for up to 5 years and to be accurate at atmospherically relevant mixing ratios to within 1% (Bertram et al., 2005).

The instrument deployed for ARCTAS had two detection cells. The direction of flow into the cell was controlled using a three-way valve and a bypass pump was used to

maintain flow in the non-sampled channel. Cell 1 sampled the ambient channel continuously while cell 2 sampled either the 180°C (50% of the time) or the 380°C channel (50% of the time). Thus for every 2 minute duty cycle there were ten 9s average measurements of NO_2, five 9s average measurements of ΣPNs, and five 9s average measurements of sum (∑PNs+∑ANs). As the ∑ANs measurement is a subtraction, the uncertainty depends both on ∑ANs and on the sum (NO_2+∑PNs). For example, if there were 100ppt each of NO_2 and ∑PNs, the precision of the ∑ANs measurement would be ~15 ppt in 20s. If there were 1 ppb each of NO_2 and ∑PNs the precision of the ∑ANs would be 40 ppt.

The TD-LIF measurement of HNO_3 has been shown to be the sum of aerosol and gas-phase HNO_3 (Fountoukis et al., 2009) and we expect aerosol phase organic nitrates to behave similarly. Comparison of TD-LIF observations of an isoprene nitrate standard to observations made using a PTR-MS show both instruments to be consistent to within 10% (Perring et al., 2009). Comparisons of NO_2 and ∑PNs have also been described and indicate similar or better accuracy for these species. (Thornton et al., 2003, Wooldridge et. al., 2009)

Observations of NO_2, □PNs and □ANs during the four ARCTAS-CARB flights and the transit flight from California to Cold Lake, Canada are shown in the Figures 1-3.

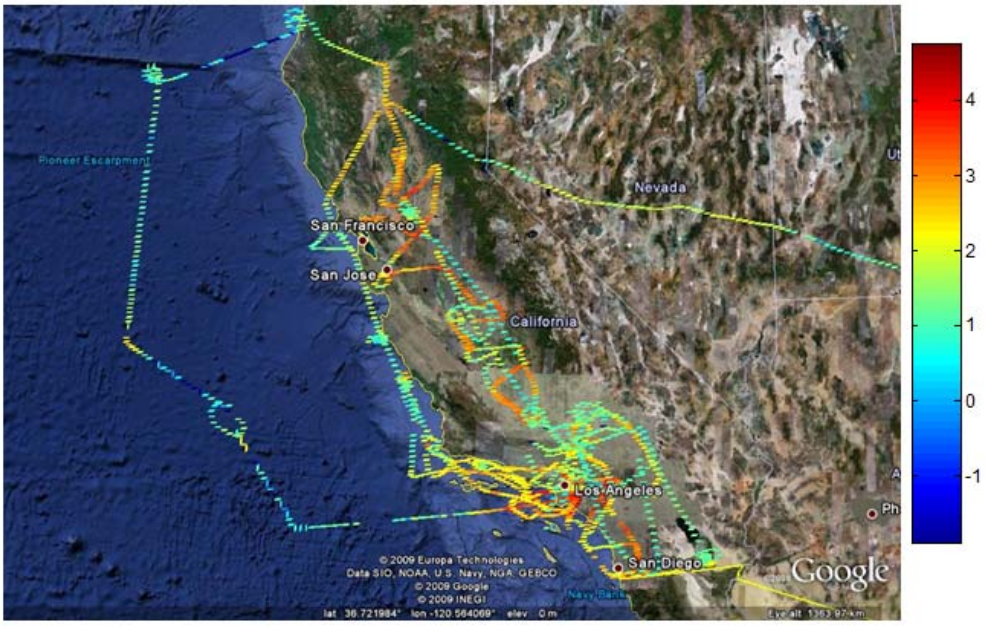

Figure 1 NO_2 measurements taken aboard the NASA DC-8 during the CARB-ARCTAS 2008
flights on June 18th, 20th, 22nd,and 24th, and on the June 26th transit flight to Cold Lake, Canada.
Scale is log(NO_2 ppt).

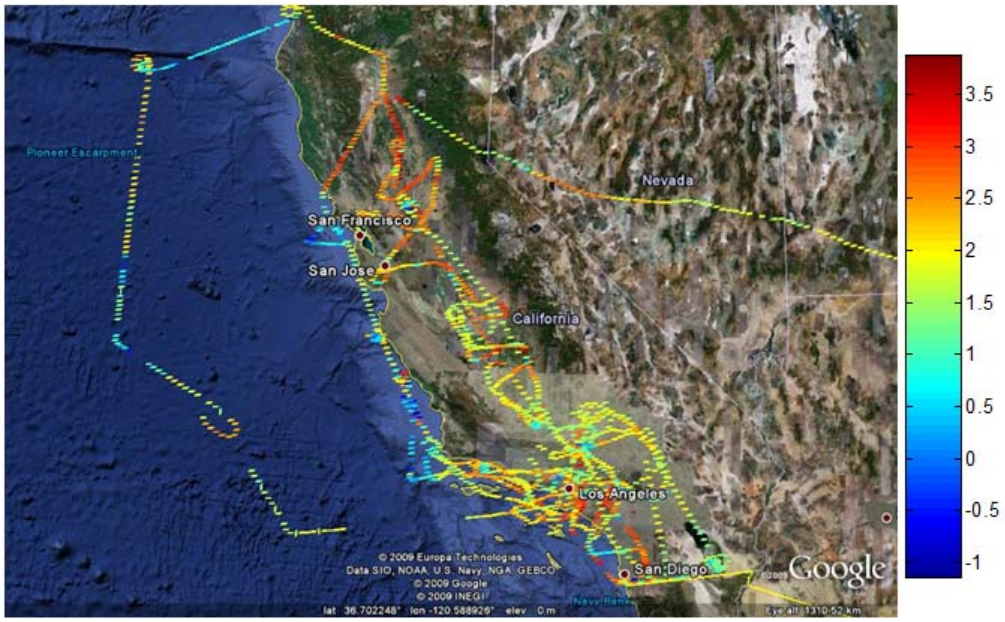

Figure 2 ΣPNs measurements taken aboard the NASA DC-8 during the CARB-ARCTAS
2008 flights on June 18th, 20th, 22nd,and 24th, and on the June 26th transit flight to Cold Lake,
Canada. Scale is log(ΣPNs ppt).

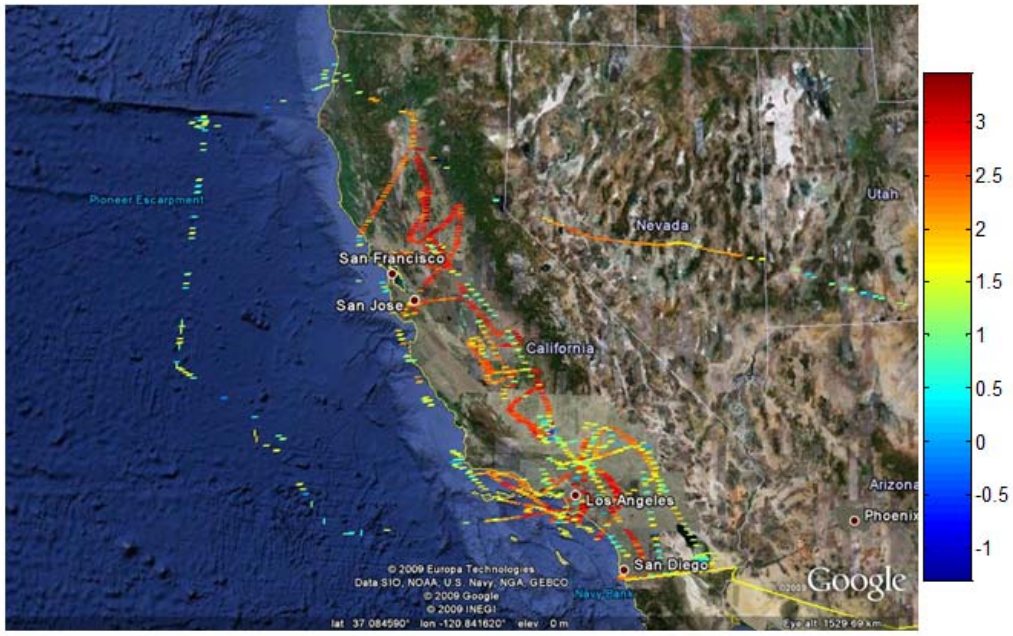

Figure 3 ΣANs measurements taken aboard the NASA DC-8 during the CARB-ARCTAS
2008 flights on June 18th, 20th, 22nd,and 24th, and on the June 26th transit flight to Cold Lake,
Canada. Scale is log(ΣANs ppt).

Task 2: Flight Planning

Flight planning was an active collaboration of DC-8 investigators, pilots and navigators and led by the CARB team. Cohen was an active participant in the discussions especially in helping to translate CARB objectives to the DC-8 community and to help to assess the capabilities of the aircraft to fly routes that were almost exclusively in the boundary layer.

Task 4: Analyses

Initial observation based analyses have been developed and results described at the ARCTAS Science team meeting and at the CARB-ARCTAS science team meeting. These analyses focus in on the role of $RONO_2$ formation as a chain termination of ozone production and on the utility of the observations as a tool to evaluate satellite NO_2 measurements.

$RONO_2$ chemistry

We observed very high ratios of $RONO_2$ to O_3 in the LA Basin. Figure 4 shows the correlation between odd oxygen (O_3+NO_2) and ΣANs for urban locations (defined at NO ≥ 10% of NO_y) in the LA Basin. Following the analysis of Rosen et. al. 2004, the inverse of the slope of this line should equal half the effective branching ratio for alkyl nitrate formation. This implies an effective branching ratio of 6% for the LA basin.

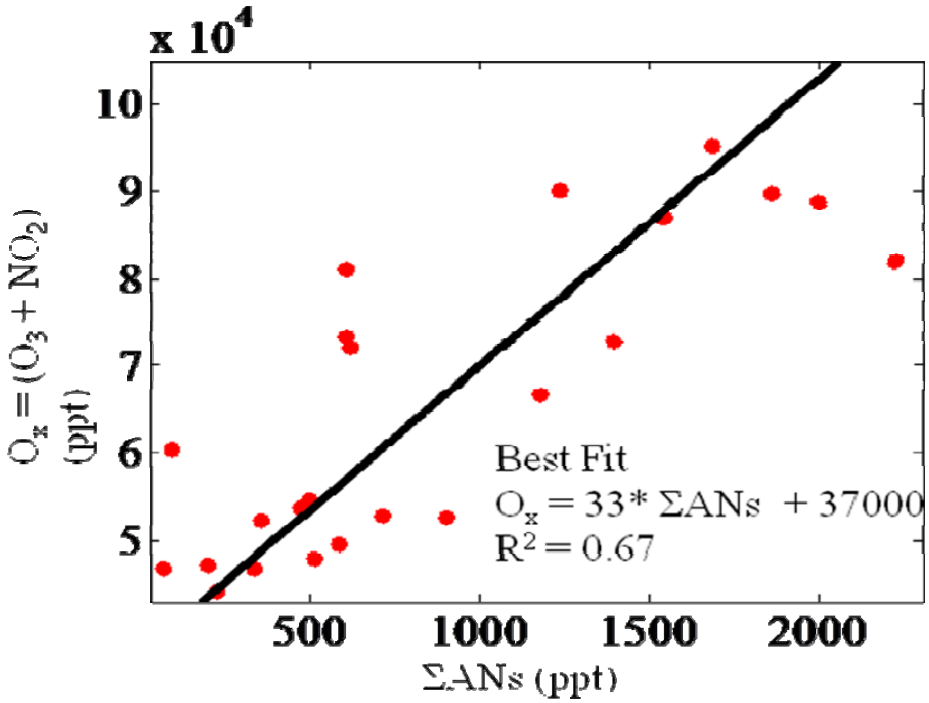

Figure 4 Correlation between O_x (= O_3 + NO_2) and total alkyl and multifunctional nitrates (ΣANs) for boundary layer measurements in urban areas of CA. Urban areas are defined as NO ≥ 10% of NO_y. The slope of this line implies a branching ration of 6% for the formation of ΣANs from urban VOC mixtures.

Satellite validation

Figures 5 and 6 show a preliminary evaluation of the comparison of boundary layer NO_2 as measured by the DC-8 with near coincident (in space and time) column NO_2 measured from the OMI instrument aboard the Aura Satellite.

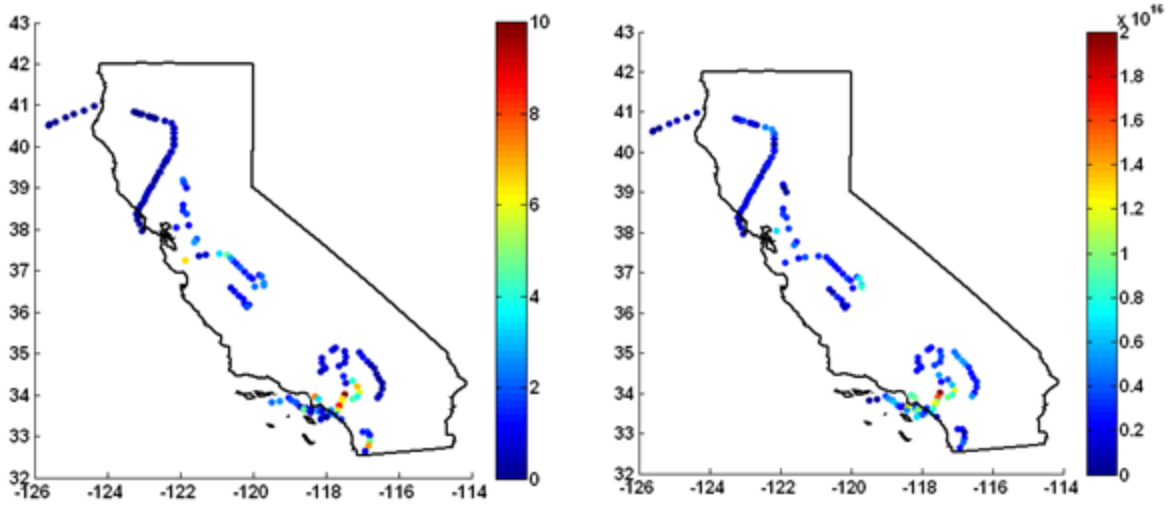

Figure 5 (Left) In-situ NO_2 (ppb) from the NASA DC-8 during the ARCTAS CARB flights. (Right) OMI tropospheric NO_2 (molecules/cm^2) for June 2008.

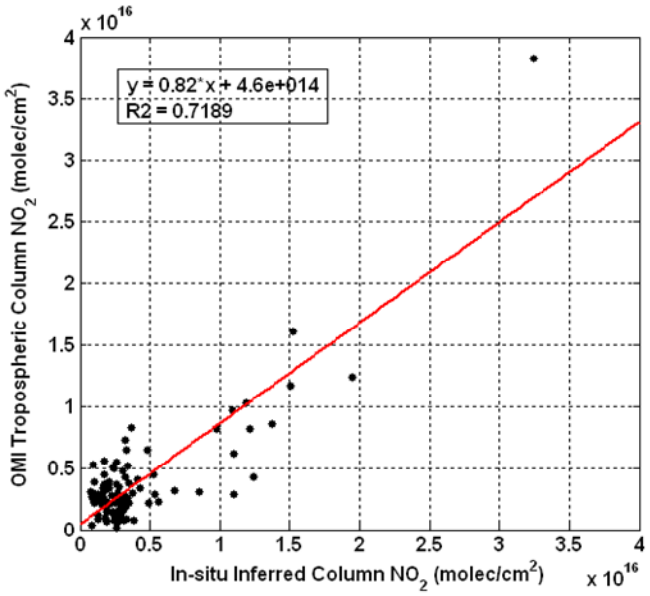

Figure 6 Correlation between the tropospheric column derived from the in-situ measurements of NO_2 aboard the NASA DC-8 and the OMI tropospheric column NO_2.

Although there remain many details to investigate, the basic pattern supports the accuracy of the OMI retrieval. As shown in figure 6, the slope of the regression in this

preliminary analysis (R^2=.72) is 0.82, possibly indicating the OMI retrievals are biased low by 18% during this season.

References

Bertram, T. H., Cohen, R. C., Thorn, W. J., and Chu, P. M., Measurement Consistency between
O_3, NO and NO_2 Standards at Tropospherically Relevant Levels, *J. Air and Waste Management Assoc.*, **55**, 1473-1479, 2005.

Cleary, P. A., Wooldridge, P. J., and Cohen, R. C., Laser-induced Fluorescence Detection of
Atmospheric NO_2 Using a Commercial Diode Laser and a Supersonic Expansion, *Applied*
Optics, **41**(33) 6950-6956, 2002.

Day, D. A., Wooldridge, P. J., Dillon, M., Thornton, J, A, and Cohen, R. C., A Thermal dissociation-laser induced fluorescence instrument for in-situ detection of NO_2, peroxy(acyl)nitrates, alkyl nitrates, and HNO_3, *J. Geophys. Res.*, **107**(D6), 10.1029/2001JD000779, 2002.

Fountoukis, C., Nenes, A., Sullivan, A., Weber, R., Van Reken, T., Fischer, M., Matias, E.,
Moya, M., Farmer, D., and Cohen, R. C., Thermodynamic characterization of Mexico City
aerosol during MILAGRO 2006, *Atmos. Chem. and Phys*., **9**, 2141-2156, 2009.

Perring, A. E., Bertram, T. H., Wooldridge, P. J., Fried, A., Heikes, B. G., Dibb, J., Crounse, J.
D., Wennberg, P. O., Blake, N. J., Brune, W. H., Blake, D. R., and Cohen, R. C., Airborne
observations of total $RONO_2$: new constraints on the yield and lifetime of isoprene nitrates,
Atmos. Chem. Phys., **9**, 1451-1463, 2009.

Rosen, R. S., Wood, E. C., Wooldridge, P. J., Thornton, J. A., Day, D. A., Kuster, W., Williams,
E. J., Jobson, B. T., and Cohen, R. C., Observations of total alkyl nitrates during Texas Air
Quality Study 2000: Implications for O_3 and alkyl nitrate photochemistry, *J. Geophys. Res.,*
109, D07303, doi:10.1029/2003JD004227, 2004.

Thornton, J. A., Wooldridge, P. J., and Cohen, R. C., Atmospheric NO_2: In Situ Laser-Induced
Fluorescence Detection at parts per trillion mixing rations, *Anal. Chem.*, **72**, 528, 2000.

Thornton, J. A., Wooldridge, P. J., Cohen, R. C., Williams, E. J., Hereid, D., Fehsenfeld, F. C.,
Stutz J., and Alicke, B., Comparison of in situ and long path measurements of NO_2 in urban
plumes, *J. Geophys. Res.*, **108**(D16), 4496, doi:10.1029/2003JD003559, 2003.

Wooldridge, P. J., Perring, A. E., Bertram, T. H., Flocke, F. M., Roberts, J. M., Singh, H. B.,
Huey, L. G., Thornton, J. A., Murphy, J. G., Fry, J. L., Rollins, A. W., LaFranchi, B. W., and
Cohen R. C., Total peroxy nitrates (ΣPNs) in the atmosphere: the thermal dissociation-laser induced fluorescence (TD-LIF) technique and comparisons to speciated PAN measurements,
Atmos. Meas. Rech. Discuss., **2**, 3055-3097, 2009.

8. Conclusions

The analysis of the volatile organic compounds measured during the ARCTAS-CARB phase highlights the presence of important emission sources within the SCAB area for many gases. We were able to identify and quantify more than 60 gases and characterize the VOC composition of different source regions within the SCAB.

Because of the increasing levels of CFC replacements in the atmosphere in the last few years, and the increasing concern on the magnitude of their contribution to global warming, we investigated the distribution of these species in greater detail. Among the HFCs, we focused our attention on HFC-152a, one of the fastest increasing CFC replacement compounds measured. Through the analysis of the HFC-152a versus CO plot we first extrapolated a HFC-152a emission of 1.0 Gg/yr from the LA County, and then used the population data to extrapolate HFC-152a emissions from the United States. This study contributes to the present knowledge of the United States' impact to the global emissions of an important greenhouse gas.

Moreover, aircraft measurements aboard the DC-8 allowed us to determine both the background level of some oxygenate in the valley as well as the enhancement level of these oxygenates when flying at low altitude through the valley. Among these compounds, we have found that ethanol, methanol, and acetaldehyde are produced in major quantities throughout the San Joaquin valley as by-products of yeast fermentation of silage and photochemical oxidation.

The data gathered during the CARB research flights were archived into the NASA website together with data obtained during the two ARCTAS deployments carried out before and after the CARB flights.

High quality nitrogen oxide measurements were submitted to a public archive. Investigations into our understanding of atmospheric chemistry using those measurements in concert with the measurements of dozens of NASA sponsored investigators are in progress.

9. References

Atlas, E., Pollock, W., Greenberg, J., Heidt, L., Thompson, A.M., 1993. Alkyl nitrates, nonmethane hydrocarbons, and halocarbon gases over the equatorial Pacific Ocean during Saga 3. Journal of Geophysical Research, [Atmospheres], 98(D9), 16933-16947.

Barletta, B., Meinardi, S. Simpson, I., Khwaja, H., Blake, D.R., Rowland, F.S., 2002. Mixing Ratios of Volatile Organic Compounds (VOCs) in the Atmosphere of Karachi, Pakistan. Atmospheric Environment, 36 3429-3443.

Berntsen, T.K., Isaksen, I.S.A., Myhre, G.. Fuglestvedt, J.S., Stordal, F., Larsen, T.A., Freckleton, R.S., Shine, K.P., 1997. Effects of anthropogenic emissions on tropospheric ozone and its radiative forcing. Journal of Geophysical Research, [Atmospheres], 102(D23), 28101-28126.

Blake, N.J., Blake, D.R., Sive, B.C., Chen, T.-Y., Rowland, F.S. Collins, J.E., Jr., Sachse, G.W., Anderson, B.E., 1996. Biomass burning emissions and vertical distribution of atmospheric methyl halides and other reduced carbon gases in the South Atlantic region. Journal of Geophysical Research, [Atmospheres], 101(D19), 24151-24164.

California Partnership for the San Joaquin Valley (CPSJV), 2007. Air Quality Action Plan. Available on-line from http://www.sjvpartnership.org/action_plan.php?wg_id=2, accessed May 20th, 2009.

Colman, J.J., Swanson, A.L., Meinardi, S., Sive, B.C., Blake, D.R., Rowland, F.S., 2001. Description of the analysis of a wide range of volatile organic compounds in whole air samples collected during PEM- Tropics A and B. Analytical Chemistry 73, 3723-3731.

Crow, D., 2005. Air Pollution Control Officer's Determination of VOC Emission Factors for Dairies. San Joaquin Valley Air Pollution Control District.

Daum, P.H., Kleinman, L.I., Springston, S.R., Nunnermacker, L.J., Lee, Y.-N., Weinstein-Lloyd, J., Zheng, J., Berkowitz, C.M., 2004. Origin and properties of plumes of high ozone observed during the Texas 2000 Air Quality Study (TexAQS 2000). Journal of Geophysical Research, [Atmospheres], 109(D17306), doi:10.1029/2003JD004311.

Greally, B.R., Manning, A.J., Reimann, S., McCulloch, A., Huang, J., Dunse, B.L., Simmonds, P.G., Prinn, R.G., Fraser, P.J., Cunnold, D.M. O'Doherty, S., Porter, L.W., Stemmler, K., Vollmer,

M.K., Lunder, C.R., Shmidbauer, N., Hermansen, O., Arduini, J., Salameh, P.K., Krummel, P.B., Wang, R.H.J., Folini, D., Weiss, R.F., Maione, M., Nickless, G., Stordal, F., Derwent, R.G., 2007. Observations of 1,1-difluoroethane (HFC-152a) at AGAGE and SOGE monitoring stations in 1994-2004 and derived global and regional emission estimates. Journal of Geophysical Research, 112, D06308, doi:10.1029/2006JD007527.

Griffin, R.J., Dabdub, D., Kleeman, M.J., Fraser, M.P., Cass, G. R., Seinfeld, J.H., 2002b. Secondary organic aerosol. 3. urban/regional scale model of size- and composition-resolved aerosols. Journal of Geophysical Research, 2002, 107, 4334.

Griffin, R.J., Dabdub, D., Seinfeld, J.H., 2002a. Secondary organic aerosol. 1. Atmospheric chemical mechanism for production of molecular constituents. Journal of Geophysical Research, 107, 4332.

Hafer, J., 2006. San Joaquin Valley Air Pollution Control District Town Hall Meeting: Ozone Plan. Discussion paper. Available on-line from http://www.valleyair.org/Town_Hall/docs/Discussion%20Paper%20July%20Town%20Hall.pdf, accessed June 19th, 2009.

Hellen, H., Kukkonen, J., Kauhaniemi, M., Laurila, T., Pietarila, H., 2005. Evaluation of atmospheric benzene concentrations in the Helsinki Metropolitan Area in 2000-2003 using diffusive sampling and atmospheric dispersion modeling. Atmospheric Environment, 39(22), 4003-4014.

Holzinger, R., C. Warneke, A. Hansel, A. Jordan, W. Lindinger, D.H. Scharffe, G. Schade, P.J. Crutzen, 1999. Biomass burning as a source of formaldehyde, acetaldehyde, methanol, acetone, acetonitrile, and hydrogen cyanide, Geophysical Research Letters, 26, 1161–1164.

Intergovernmental Panel on Climate Change (IPCC) 2001. Houghton, J.T., et al. (Eds), Climate Change 2001 – The Scientific Basis. Cambridge, UK, 2001.

Kleinman, L.I., Daum, P.H., Imre, D., Lee, Y.-N., Nunnermacker, L.J., Springston, S.R., Weistein-Lloyd, J., Rudolph, J., 2002. Ozone production rate and hydrocarbon reactivity in 5 urban areas: a cause of high ozone concentration in Houston. Geophysical Research Letters, 29(10), 105/1-105/4.

Lin, T.Y., Sree, U., Tseng S.H., Chiu, K.H., Wu, C.H., Lo, J.G., 2004. Volatile organic compound concentrations in ambient air of Kaohsiung petroleum refinery in Taiwan. Atmospheric Environment, 38(25), 4111-4122.

Lindberg, J. 2007. Analysis of the San Joaquin Valley 2007 Ozone Plan. State of California Air Resources Board. Final Draft Staff Report.

McCulloch, A., Ashford, P., and Midgley, P.M., 2001. Historic emissions of fluorotrichloromethane (CFC-11) based on a market survey. Atmospheric Environment, 35(26), 4387-4397.

McCulloch, A., Aucott, M.L., Benkovitz, C.M., Graedel, T.E., Kleiman, G. Midgley, P.M., Li, Y.-F., 1999. Global emissions of hydrogen chloride and chloromethane from coal combustion, incineration and industrial activities: Reactive Chlorine Emissions Inventory. Journal of Geophysical Research, [Atmospheres], 104(D7), 8391-8403.

McCulloch, A., Midgley, P.M., Ashford, P., 2003. Releases of refrigerant gases (CFC-23, HCFC-22 and HFC-134a) to the atmosphere. Atmospheric Environment, 37(7), 889-902.

McDaniel, D., 2005. Clean Air – Collaborating to Reduce Diesel Emissions. Region 9: 2005 Progress Report. US EPA. Available on-line from http://www.epa.gov/region09/annualreport/05/air.html, accessed June 18th, 2009.

O'Doherty. S., P.G. Simmonds, and G. Spain, 2008. Advanced Global Atmospheric Gases Experiment – Annual Report. University of Bristol. Project No. GA01081. Available on-line from http://209.85.173.132/search?q=cache:K68qfEAKGu4J:randd.defra.gov.uk/Document.aspx%3FDocument%3DGA0201_7766_ANN.doc+C2Cl4+lifetime+in+the+atmosphere&cd=21&hl=en&ct=clnk&gl=us&client=safari, accessed May 13, 2009.

Owen, J., 2005. California Cows Fail Latest Emissions Test. National Geographic News. Available on-line from http://news.nationalgeographic.com/news/2005/08/0816_050816_cowpollution.html, accessed June 18th, 2009.

Placet, M., Mann, C.O., Gilbert, R.O., Niefer, M.J., 2000. Emissions of ozone precursors from stationary sources: a critical review. Atmospheric Environment, 34(12-14), 2183-2204.

Quack, B., and Wallace, D.W.R., 2003. Air-sea flux of bromoform: Controls, rates, and implications. Global Biogeochemical Cycles, 17(1), 1023, doi:10.1029/2002GB001890.

Sachse, G., G. Hill, L. Wade, and M. Perry, 1987. Fast-Response, High-Precision Carbon Monoxide Sensor Using a Tunable Diode Laser Absorption Technique, Journal of Geophysical Research, 92(D2), 2071–2081.

Shine, K.P., 2001. Atmospheric ozone and climate change. Ozone: Science & Engineering,, 23(6), 429-435.

Simpson, I. J., S. Meinardi, N. J. Blake, F. S. Rowland, and D. R. Blake, 2004. Long-term decrease in the global atmospheric burden of tetrachloroethene (C2Cl4). Geophysical Research Letters, 31, L08108, doi:10.1029/2003GL019351.

Singh, H.B., Salas, L.J., Chatfield, R.B., Czech, E., Fried, A., Walega, J., Evans, M.J., Field, B.D., Jacob, D.J., Blake, D., Heikes, B., Talbot, R., Sachse, G., Crawford, J.H., Avery, M.A., Sandholm, S., and Fuelberg, H., 2004. Analysis of the atmospheric distribution, sources, and sinks of oxygenated volatile organic chemicals based on measurements over the Pacific during TRACE-P. Journal of Geophysical Research, [Atmospheres], 109(D15S07), doi:10.1029JD2003003883.

Smith, L., 2008. California Ambient Air Quality Standards (CAAQS). California Air Resources Board. Available on-line from http://www.arb.ca.gov/research/aaqs/caaqs/caaqs.htm, accessed May 25th, 2009.

Stoddard, E., 2009. FACTBOX: Water scarcity and agriculture in California. Thomson Reuters 2009. Available on-line from http://www.reuters.com/article/environmentNews/idUSTRE52C08M20090313, accessed June 17th, 2009.

Stohl, A., Seibert, P.,Arduini, J., Eckhardt, S., Fraser, P., Greally, B.R., Lunder, C., Maione, M., Muhle, J., O'Doherty, S., Prinn, R.G., Reimann, S., Saito, T., Schmidbauer, N., Simmonds, P.G., Vollmer, M.K., Weiss, R.F., Yokouchi, Y., 2009. Atmospheric Chemistry and Physics, 9, 1597-1620.

Sturrock, G.A., Etheridge, D.M., Trudinger, C.M., Fraser, P.J., Smith, A.M., 2002. Atmospheric histories of halocarbons from analysis of Antarctic firn air: Major Montreal Protocol species. Journal of Geophysical Research, [Atmospheres], 107(D24), 4765-4778.

Swanson, A.L., Davis, D.D., Arimoto, R., Roberts, P., Atlas, E.L., Flocke, F., Meinardi, S., Sherwood R.F., and Blake, D.R., 2004. Organic trace gases of oceanic origin observed at South Pole during ISCAT 2000. Atmospheric Environment, 38(32), 5463-5472.

United Nations Environment Programme (UNEP), 2003 United Nations Environment Programme (UNEP), 2003. Handbook for the International treaties for the protection of the ozone layer. Nairobi, Kenya.

United States Environmental Protection Agency, 2009. Ground level Ozone. Available on-line from http://www.epa.gov/air/ozonepollution/actions.html#mar07s, accessed June 17th, 2009.

University of Maryland, Baltimore County (UMBC). U.S. Air Quality: The Smog Blog. Available on-line from http://alg.umbc.edu/usaq/archives/2008_06.html, accessed May 11th, 2009.

Vingarzan, R., 2004. A review of surface ozone background levels and trends. Atmospheric Environment, 38(21), 3431-3442.

Watson, J.G., Chow, J.C., Fujita, E.M., 2001. Review of volatile organic compound source apportionment by chemical mass balance. Atmospheric Environment, 35(9), 1567-1584.

World Meteorological Organization (WMO), 2002 World Meteorological Organization (WMO), 2002. Scientific assessment of ozone depletion: 2002. Global Ozone Research and Monitoring Project—Report No. 47, Geneva, Switzerland.